FRA-75-22

REPORT NO. FRA-OR&D-76-277

ULTRASONIC DETECTION OF PLATE CRACKS IN RAILWAY WHEELS

F.L. Becker

Batelle
Pacific Northwest Laboratories
Richland WA 99352

JULY 1976

FINAL REPORT

Prepared for

U.S. DEPARTMENT OF TRANSPORTATION
FEDERAL RAILROAD ADMINISTRATION
Research and Development
Washington DC 20590

Technical Report Documentation Page

1. Report No.	2. Government Accession No.	3. Recipient's Catalog No.
FRA-OR&D-76-277		

4. Title and Subtitle	5. Report Date
ULTRASONIC DETECTION OF PLATE CRACKS IN RAILWAY WHEELS	July 1976
	6. Performing Organization Code
7. Author(s)	8. Performing Organization Report No.
F.L. Becker*	DOT-TSC-FRA-75-22
9. Performing Organization Name and Address	10. Work Unit No. (TRAIS)
Battelle Pacific Northwest Laboratories Richland WA 99352	RR628/R6316
	11. Contract or Grant No. DOT-TSC-726
12. Sponsoring Agency Name and Address	13. Type of Report and Period Covered
U.S. Department of Transportation Federal Railroad Administration Research and Development Washington DC 20590	Final Report January 1973-May 1974
	14. Sponsoring Agency Code

15. Supplementary Notes	
*Under contract to:	U.S. Department of Transportation Transportation Systems Center Kendall Square Cambridge MA 02142

16. Abstract

The results of experimental efforts established the feasibility of the detection of railway wheel plate cracks by an ultrasonic pulse echo testing technique from the tread surface.

Feasibility and test sensitivities were established using artificial notches in a flat plate test reference and in full-size wheels.

Concepts for manual inspection of stationary wheels and the automatic testing of moving wheels are described.

Recommendations for further development are included.

17. Key Words	18. Distribution Statement
Railway Wheels Flaw Detection Ultrasonic Plate Cracks	DOCUMENT IS AVAILABLE TO THE PUBLIC THROUGH THE NATIONAL TECHNICAL INFORMATION SERVICE, SPRINGFIELD, VIRGINIA 22161

19. Security Classif. (of this report)	20. Security Classif. (of this page)	21. No. of Pages	22. Price
Unclassified	Unclassified	88	

Form DOT F 1700.7 (8-72) Reproduction of completed page authorized

PREFACE

This report summarizes a study conducted by Battelle Pacific Northwest Laboratories (Battelle Northwest) for the Department of Transportation, under Contract No. DOT-TSC-726. The principal investigator was F.L. Becker, of the Physics and Instrumentation Department, Nondestructive Testing Section. Contributions were made by G.J. Posakony and S.J. Foreman, Battelle Northwest.

Acknowledgement is made of the assistance of:

D.E. Bray, formerly of DOT-FRA

R.K. Steele, DOT-TSC

D.H. Stone, AAR

Abex Corporation

Atchison, Topeka and Santa Fe Railway Company

Bethlehem Steel Corporation

Chicago, Rock Island, and Pacific Railroad Company

Griffin Wheel

Missouri Pacific Railroad Company

Seaboard Coast Line Railroad Company

Southern Pacific Transportation Company

Southern Railway System

Toronto Transit Commission

METRIC CONVERSION FACTORS

Approximate Conversions to Metric Measures

Symbol	When You Know	Multiply by	To Find	Symbol
		LENGTH		
in	inches	2.5	centimeters	cm
ft	feet	30	centimeters	cm
yd	yards	0.9	meters	m
mi	miles	1.6	kilometers	km
		AREA		
in^2	square inches	6.5	square centimeters	cm^2
ft^2	square feet	0.09	square meters	m^2
yd^2	square yards	0.8	square meters	m^2
mi^2	square miles	2.6	square kilometers	km^2
	acres	0.4	hectares	ha
		MASS (weight)		
oz	ounces	28	grams	g
lb	pounds	0.45	kilograms	kg
	short tons (2000 lb)	0.9	tonnes	t
		VOLUME		
tsp	teaspoons	5	milliliters	ml
Tbsp	tablespoons	15	milliliters	ml
fl oz	fluid ounces	30	milliliters	ml
c	cups	0.24	liters	l
pt	pints	0.47	liters	l
qt	quarts	0.95	liters	l
gal	gallons	3.8	liters	l
ft^3	cubic feet	0.03	cubic meters	m^3
yd^3	cubic yards	0.76	cubic meters	m^3
		TEMPERATURE (exact)		
°F	Fahrenheit temperature	5/9 (after subtracting 32)	Celsius temperature	°C

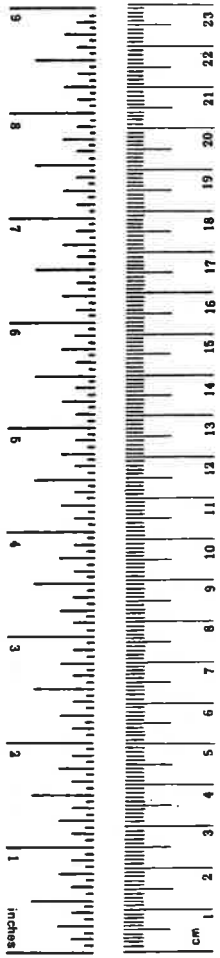

Approximate Conversions from Metric Measures

Symbol	When You Know	Multiply by	To Find	Symbol
		LENGTH		
mm	millimeters	0.04	inches	in
cm	centimeters	0.4	inches	in
m	meters	3.3	feet	ft
m	meters	1.1	yards	yd
km	kilometers	0.6	miles	mi
		AREA		
cm^2	square centimeters	0.16	square inches	in^2
m^2	square meters	1.2	square yards	yd^2
km^2	square kilometers	0.4	square miles	mi^2
ha	hectares (10,000 m^2)	2.5	acres	
		MASS (weight)		
g	grams	0.035	ounces	oz
kg	kilograms	2.2	pounds	lb
t	tonnes (1000 kg)	1.1	short tons	
		VOLUME		
ml	milliliters	0.03	fluid ounces	fl oz
l	liters	2.1	pints	pt
l	liters	1.06	quarts	qt
l	liters	0.26	gallons	gal
m^3	cubic meters	35	cubic feet	ft^3
m^3	cubic meters	1.3	cubic yards	yd^3
		TEMPERATURE (exact)		
°C	Celsius temperature	9/5 (then add 32)	Fahrenheit temperature	°F

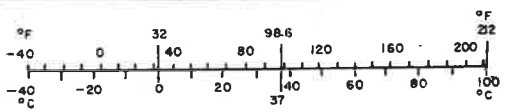

TABLE OF CONTENTS

LIST OF ILLUSTRATIONS

LIST OF ILLUSTRATIONS (CONTINUED)

LIST OF ILLUSTRATIONS (CONTINUED)

LIST OF ABBREVIATIONS AND SYMBOLS

A_n	Nth asymmetric Lamb mode
BFN1	Back face rim fillet to plate transition (see Figure 17)
d	Plate thickness
DAC	Distance amplitude correction
F	Frequency
Fd	Product of frequency and plate thickness
FFN2	Front face hub fillet to plate transition (see Figure 17)
L	Indicating longitudinal wave propagation
r	Radius of an ultrasonic transducer
s	Spacing between multiple signals produced by shear wave multiples in plate propagation
S_N	Nth symmetric Lamb mode
V_L	Velocity of longitudinal waves
V_P	Phase velocity
V_t	Velocity of shear waves
Z	Acoustic impedance, product of density and velocity
λ	Wavelength of an ultrasonic wave (v/F)
ϕ	Dispersion half angle produced by an ultrasonic transducer, measured from the transducer center line
ρ	Density
σ_1	Circumferential (hoop) stress on wheel plate
σ_2	Radial stress on wheel plate
θ	Angle of incidence, reflection or refraction, measured from a normal to the surface.

EXECUTIVE SUMMARY

THE PROGRAM AND TECHNIQUES EMPLOYED

The steadily increasing loads and speeds experienced by railway cars in recent years have been accompanied by an increased incidence of wheel failures.[1][2] Cost effective, simple and reliable testing procedures for early detection of defects in railway wheels could substantially reduce the number of these failures. This document presents the results of experimental efforts to establish the feasibility of detecting plate cracks in railway wheels by ultrasonic techniques.

The long-range goal of this program is to develop procedures and systems capable of detecting wheel-plate cracks while the equipment is in the shop or on moving cars. The immediate objective was to explore the feasibility of ultrasonic pulse-echo techniques requiring access to the tread surface only, since this is the only surface that is readily accessible and usually clean. In particular, it was desired to extend previous investigations by D.E. Bray[3] which indicated that excitation of Lamb waves in the plate region (by means of incident longitudinal waves of appropriate direction and frequency) might offer significant advantages for such testing.

The scope of this program included:

1. Development of the most suitable ultrasonic pulse-echo technique.
2. Demonstration of the sensitivity of the technique on five typical wheel configurations.
3. Preparation of recommendations for further development of systems for manual inspection of stationary wheels and fully automated inspection of the wheels under moving cars.

The two techniques investigated in this study utilize longitudinal ultrasonic waves introduced from the tread surface. In the first or "Lamb mode" technique, a resonant plate wave was generated

at prescribed combinations of plate thicknesses and frequencies. By selecting optimum modes of propagation (to match the plate thickness), relatively high flaw sensitivities can be achieved over considerable distances. In the second or "Longitudinal-Shear Wave" technique, shear waves were generated by mode conversions of the incident longitudinal wave, upon reflection from the plate surfaces. Reflections of these longitudinal and shear waves from defects were then detected by the transmitting transducer located on the tread surface.

Section 2 of this report describes these techniques and their basic capabilities, as established by using a 1-inch thick test plate with machined notches of various depths. The application of both techniques to full size wheels with natural and simulated defects is described in Section 3. The second or Longitudinal-Shear Wave technique proved to be the most suitable test method because of a higher signal-to-noise ratio and its higher sensitivity to defects located in the back rim fillet. After the superiority of the Longitudinal-Shear Wave technique had been demonstrated early in the program, further effort on the Lamb wave technique was discontinued.

The smallest defects and notches available during wheel testing were 1.5-inch long, 0.125-inch deep machined notches. Notches located in the back rim fillets of the B-28, J-33, CJ-33, H-36 and M-33 wheels were easily detectable by the Longitudinal-Shear Wave technique. Hub-fillet notches were also easily detectable in all but the 2-wear, M-33 wheel. The reason for lack of hub notch sensitivity has not yet been determined. With the exception of the M-33 hub defects, we estimate that the smallest defects which could be detected are rim fillet defects 0.22-inch long by 0.07-inch deep, and hub fillet defects 0.3-inch long by 0.1-inch deep.

System concepts or preferred embodiments of the Longitudinal-Shear Wave technique are described for manual and automatic testing applications. In the manual system, the inspector would use a small battery-operated ultrasonic instrument and a specially designed ultrasonic transducer with a self-contained couplant supply. Scanning the entire circumference of the wheel is required for a

complete inspection, since maximum sensitivity is achieved when the transducer is directly over the flaw. This would require a rotation of the wheel or movement of the car, to achieve 100-percent inspection. The manual technique could be used to good advantage in the wheel shop for spot checking of groups of wheels suspected to be prone to failure and for the verification of defects detected by the automatic testing systems.

One possible automatic testing system concept consists of two test rail sections each containing up to 40 transducers and a multi-channel electronic system. Each wheel is inspected as it rolls over the series of transducers at speeds between 10 to 20 mph. With 40 transducers spaced 3 inches apart, the system would detect 95 to 100 percent of all wheel plate defects of 1 inch in length or greater and 75 percent of defects between 0.4 and 1.0 inches long. The detection probability could be increased by decreasing the transducer spacing and increasing the number of transducers. The system should be capable of substantially reducing the occurrence of accidents resulting from wheel failure, at a reasonable cost. At this stage of development, it is difficult to predict costs accurately; it is however, expected that the inspection cost per wheel could range from 0.1 to 0.9 cents per wheel (including capital operating and maintenance costs) and would depend on the number of cars tested per day.

The manual inspection technique can be applied in the field with a minimum of further development. The required development would consist mainly of modifications and improvements in the transducer and electronic detection system. A field evaluation program of the manual technique on a wide range of wheel types and conditions would provide a large body of information on which the development of the automatic system could be based. The automatic test system would require considerably more development before it could be applied in the field. For this reason, it must be recommended that a short section of test rail (10 or more transducers) and a suitable electronic system be developed. This test rail section would be used to verify the capabilities of the technique in the laboratory and later could be installed in a test track for

evaluation under operating conditions. Full scale systems could be developed from the resulting experience.

Consequently, it is the belief of the researchers that this ultrasonic technique promises to be an effective wheel-plate crack detection method that will provide for a timely removal of faulty wheels, thus preventing many of the prevalent serious accidents caused by wheel failure.

1. INTRODUCTION

APPROACH TO WHEEL PLATE TESTING

Cost effective, simple and reliable testing prodecures for early detection of defects in railway wheels could substantially reduce the number of service-related failures. The increased incidence of wheel failures[1] in recent years is attributed to the steadily increasing loads and speeds experienced by railway cars. In 1971 and 1972, 1279 reported accidents were attributable to wheel and axle failures, resulting in $37,486,304 damage to railroad property.[1] If cargo damage were added, the actual loss due to this type of accident would likely double or triple. Approximately half of these accidents involved wheel failures. The American Association of Railroads (AAR) reports that 24 percent of the wheel failures during 1972 were of the cracked plate type.[2] If we assume that cargo damage is roughly equivalent in cost to equipment damage, we estimate that wheel plate failures have caused approximately $4.5 million in annual losses. This justifies the development of non-destructive inspection techniques capable to ensure substantial reduction of incidents caused by wheel plate failures. However, to be cost effective, the inspection costs per wheel would need to be low (i.e., less than 1¢ per wheel), there being approximately 15 million wheels in the rail service.

Railway car wheel plate failures due to service stresses generally occur at the front hub or rear rim fillets. Stresses in the wheel result from rotational energy, the static support of the car load, the dynamic load associated with train motion and track profile, and plastic distortion of the rim due to the high rim temperatures generated by tread braking. The cyclic nature of dynamic load application during wheel rotation also contributes to failure by fatigue. Thermal stresses due to prolonged brake application can reach very high levels which also cause failures. Figure 1 shows the stresses resulting from a simulated brake drag test lasting 8 minutes.[4] Radial surface stresses on this wheel exceed 50 ksi at the front hub fillet-to-plate transition (FFN2)

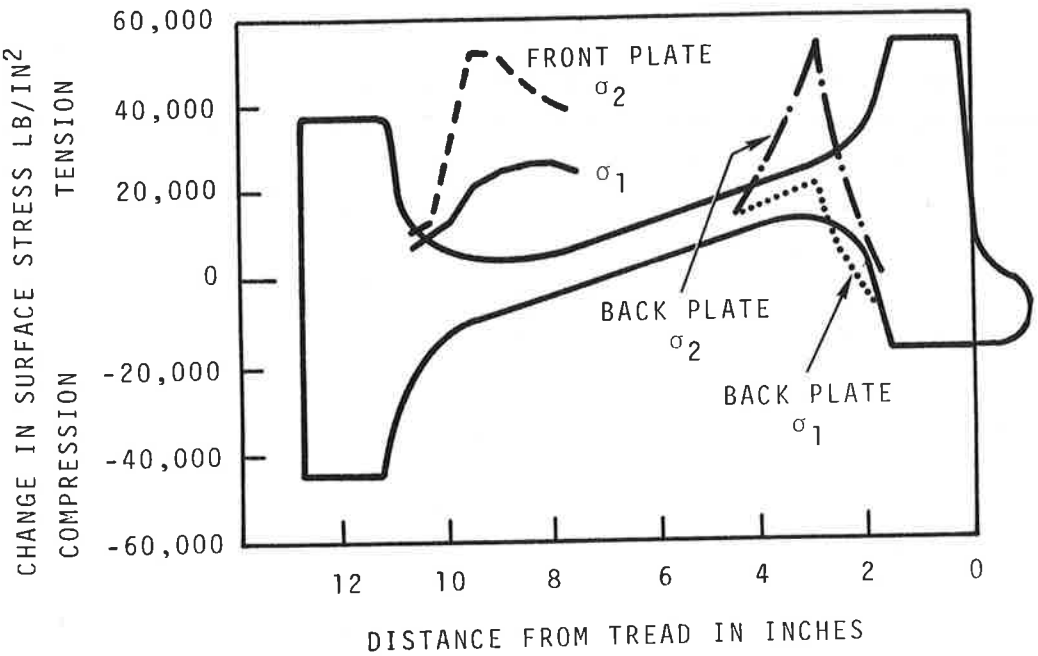

NOTES

1. Drag duration = 8 min. at 25 KW
2. σ_1 = Circumferential stress.
3. σ_2 is perpendicular to σ_1 measured along wheel contour.
4. Also refer to Ref. 4.

Figure 1. Surface Stresses on a Straight-Plate, Sharp-Fillet Wheel Subjected to a Simulated Drag Test

and at the back rim fillet-to-plate transition (BFN1). Dynamic track loading conditions also result in maximum radial tensile stresses at the front hub fillet.[5] As seen from the above data, it is not surprising that wheel plate failures predominantly occur in these two locations[6] (FFN2 and BFN1). Thus, a concentrated inspection effort to detect cracks at the two locations becomes feasible.

The long-range goal of this program has been projected as development of procedures and systems capable of detecting wheel-plate cracks, while the wheels are in the shop or under moving cars. The immediate objective was to explore the feasibility of pulse-echo techniques requiring access to the tread surface only, since this is the only surface readily accessible and usually clean. In particular, it was desired to extend previous investigations by D.E. Bray,[3] which had indicated that excitation of Lamb waves in the plate region (by means of incident longitudinal waves of appropriate direction and frequency) might offer significant advantages for such testing.

The advantages and disadvantages of the Lamb-mode approach, as compared to more conventional techniques employing higher frequencies, were experimentally explored in this program. Both approaches are described and evaluated in Section 2 with respect to their detection sensitivity for calibration notches in a flat test plate simulating the defects that might be encountered in a wheel plate. Section 3 presents the results obtained with both techniques on full-size wheels containing both service-induced and simulated defects. The relative merits and capabilities of the two techniques are then discussed, and concepts are advanced for systems, both for manual inspection of stationary wheels and for automated inspection of wheels on moving cars in service.

2. TEST METHOD

2.1 DEFINITION OF TECHNIQUES

The two testing techniques described in this report are designated as the "Lamb Wave" and "Longitudinal-Shear Wave". The Lamb waves are a specialized form of plate waves which can occur for specific combinations of frequencies and plate thickness. A brief description of the nature and properties of Lamb wave is contained in a following paragraph.

The frequencies and pulse lengths used in the Longitudinal-Shear Wave technique do not meet the specific requirements for Lamb mode generation. Propagation within the plate in the Longitudinal-Shear Wave technique is a combination of incident longitudinal wave and mode-converted shear waves. The basic sensitivity of each method was evaluated using a flat standard test plate containing artificial notches of various depths. Application of these test methods to full-size wheels is discussed in Section 3.

2.2 LAMB WAVE TECHNIQUE

Lamb first presented his theory[7] of plate wave propagation in 1917. Since that time, several researchers have used such waves for the detection of defects in thin plates.[8-10] An exhaustive theoretical presentation on the nature of Lamb waves is not attempted here, as several comprehensive dissertations by Viktorov,[11] Redwood,[12] and Worlton[13] are contained in the readily available literature (see References at the end of this document). However, the nature of Lamb waves is discussed to give the reader a basic understanding of this propagation mode.

Lamb waves are a unique combination of dilational (i.e., longitudinal) and transverse (i.e., shear) waves propagating in a plate. As each of these waves strikes the boundary of the plate they are mode-converted (longitudinal to shear, and shear back to longitudinal) and reflected at angles determined by Snell's law, as shown in Figure 2. There are a number of unique combinations of

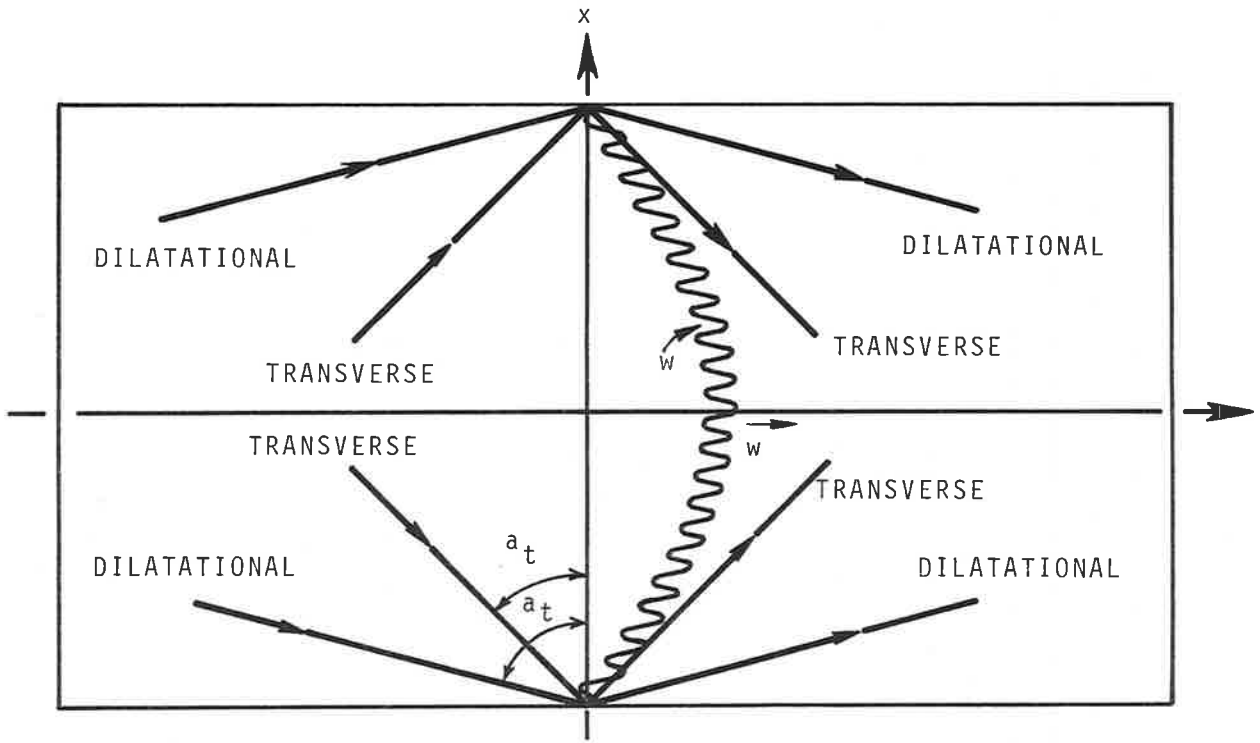

Figure 2. Synthesis of a Wave Mode in a Plate[11]

incident angles, plate thicknesses, and frequencies or wavelengths where the phase of each wave reinforces the other, producing the plate displacement patterns shown in Figure 3. These are preferred modes of propagation and dissipate only through attenuation or reflection from a discontinuity in the plate.

Two modes producing elliptical displacements are possible: symmetrical and asymmetrical. The symmetrical modes are characterized by symmetrical displacements around the centerline of the plate, while asymmetric modes exhibit asymmetrical displacements. The normal and tangential components of these displacements are not uniform throughout the plate thickness, but vary from zero to a maximum one or more times, depending on the mode and the product of frequency and plate thickness (Fd). This fact is very useful in testing, because it permits the selection of a mode which has maximum sensitivity for a specific defect.

Lamb waves exhibit two characteristic velocities: phase velocity and group velocity. Phase velocity is the velocity of a displacement crest measured past a fixed observer. The wave length shown in Figure 3 is associated with this phase velocity. Group velocity is the velocity of energy propagation in the plate which would be measured in pulse-echo testing. Calculated phase and group velocities for steel are shown in Figures 4 and 5, for symmetrical modes, and in Figures 6 and 7 for asymmetrical modes. Each mode numbered 1.0 or larger has a lower cutoff Fd product, below which the mode cannot exist. At this critical Fd product, the group velocity approaches zero, and the phase velocity asymptotically approaches infinity, indicating a standing wave. Note that the group velocity never exceeds the longitudinal velocity and that both group and phase velocity asymptotically approach the surface-wave velocity for large Fd products.

Lamb waves can be generated by several methods. The most common of these is the technique of using longitudinal waves obliquely incident on the plate surface. A Lamb mode is generated when the phase velocity (V_p) of the incident waves matches that of the Lamb mode at the Fd product. The phase velocity of the incident wave is given by

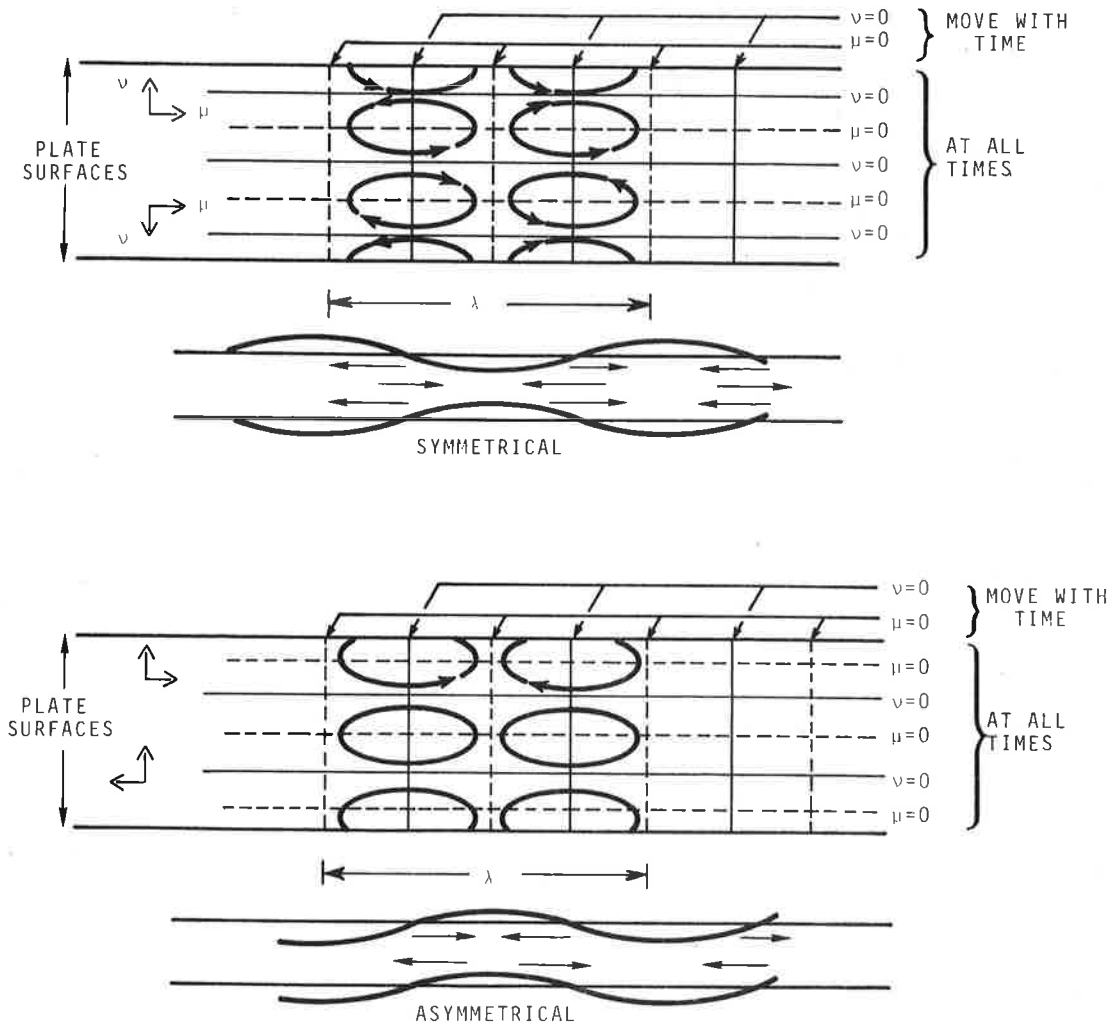

Figure 3. Particle Motions Corresponding to Symmetrical and Asymmetrical Waves (12)

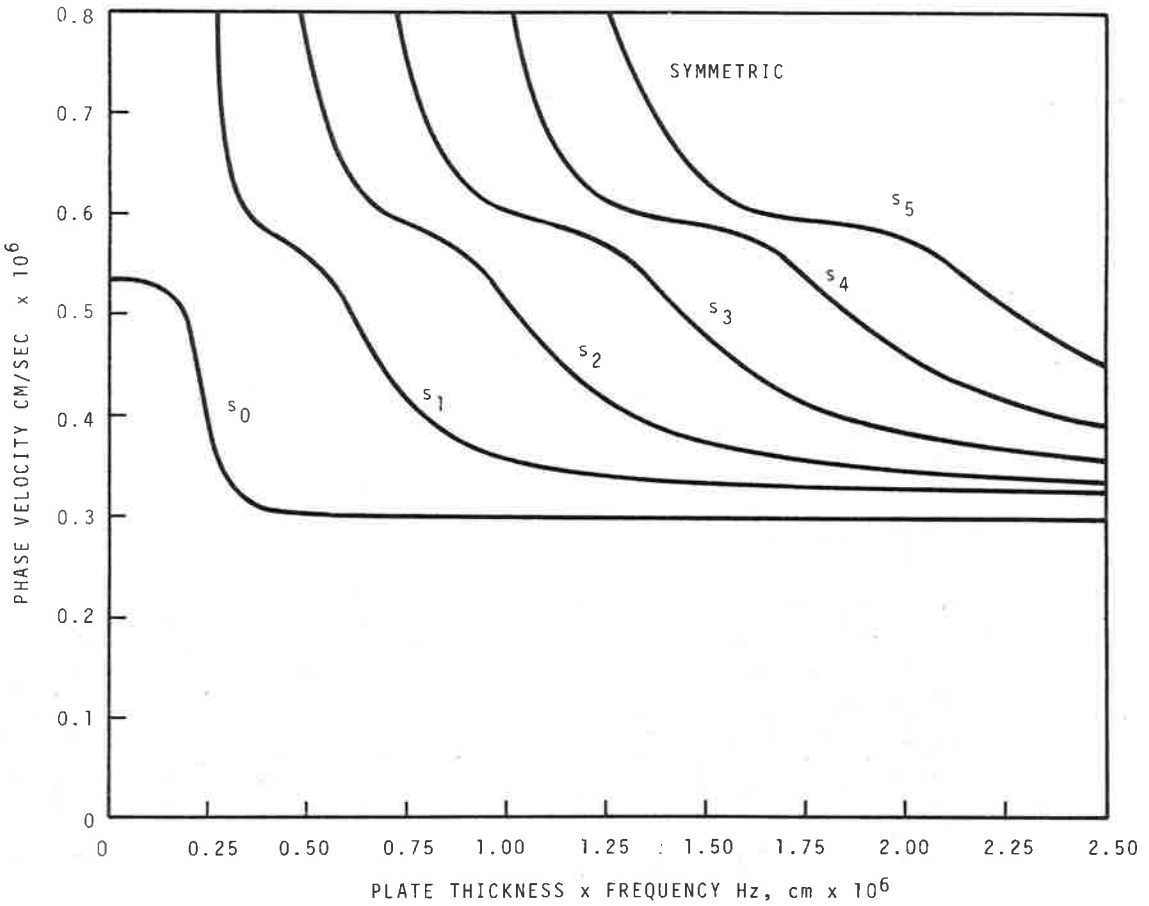

NOTES:

1. Longitudinal velocity = 5.96×10^5 cm/sec.
2. Shear wave velocity = 3.26×10^5 cm/sec.

Figure 4. Phase Velocities for Symmetrical Lamb Modes in Steel

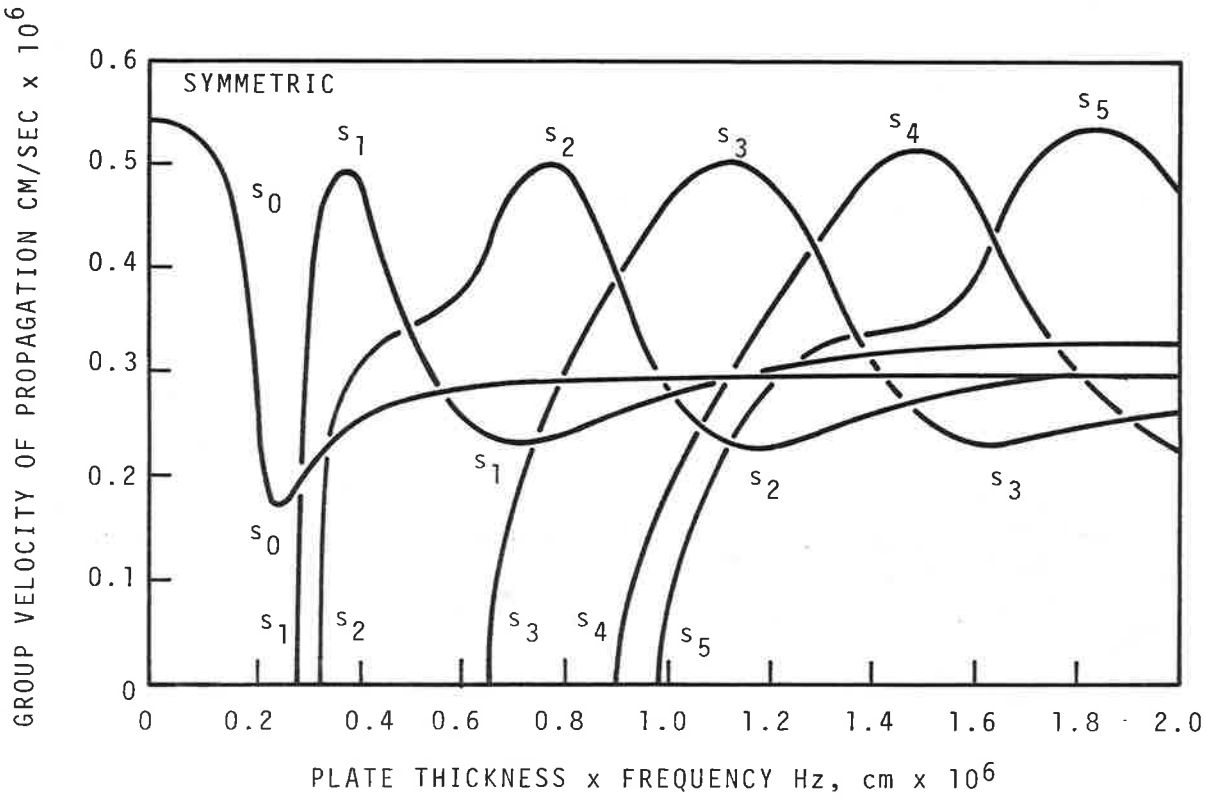

Figure 5. Group Velocities for Symmetrical Lamb Modes in Steel

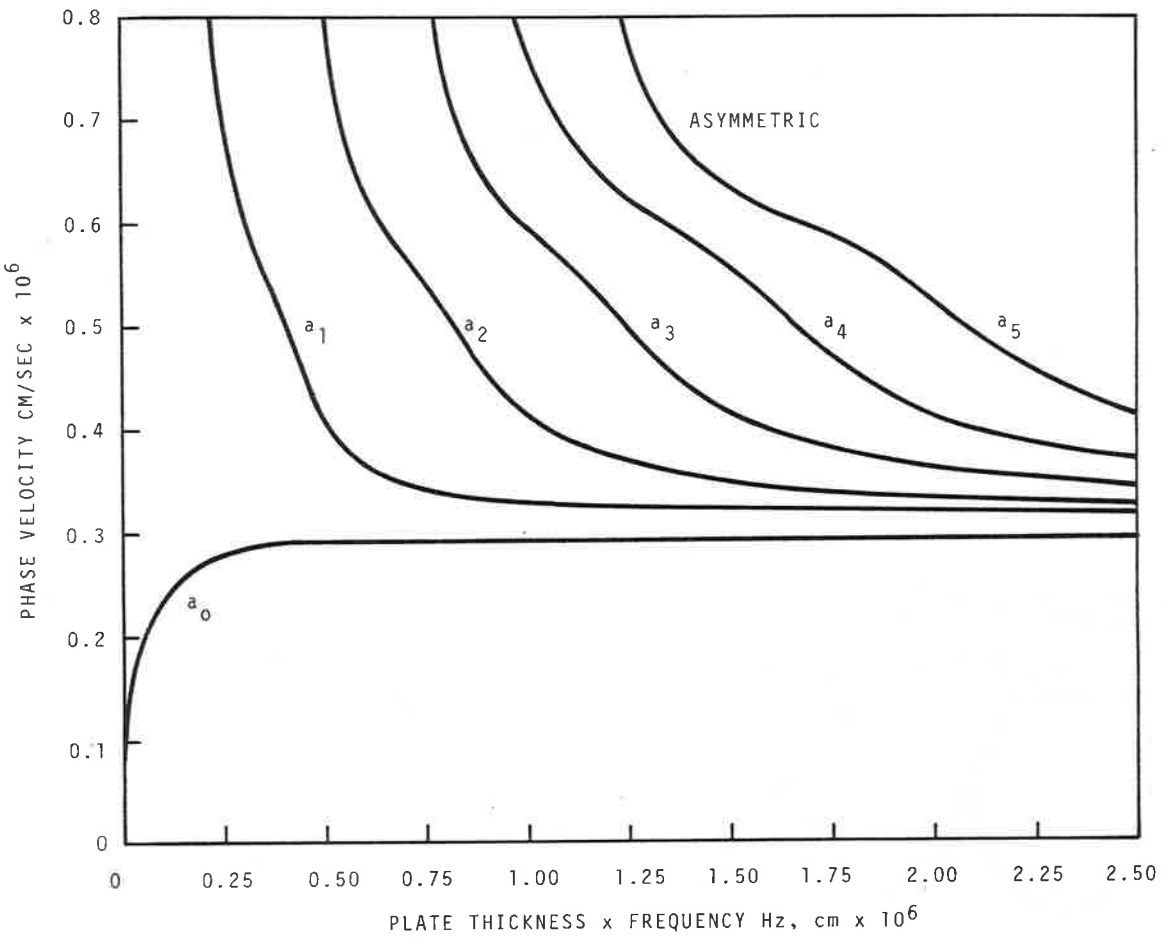

NOTES:

1. Longitudinal velocity = 5.96×10^5 cm/sec.
2. Shear wave velocity = 3.26×10^5 cm/sec.

Figure 6. Phase Velocities for Asymmetrical Lamb Modes in Steel

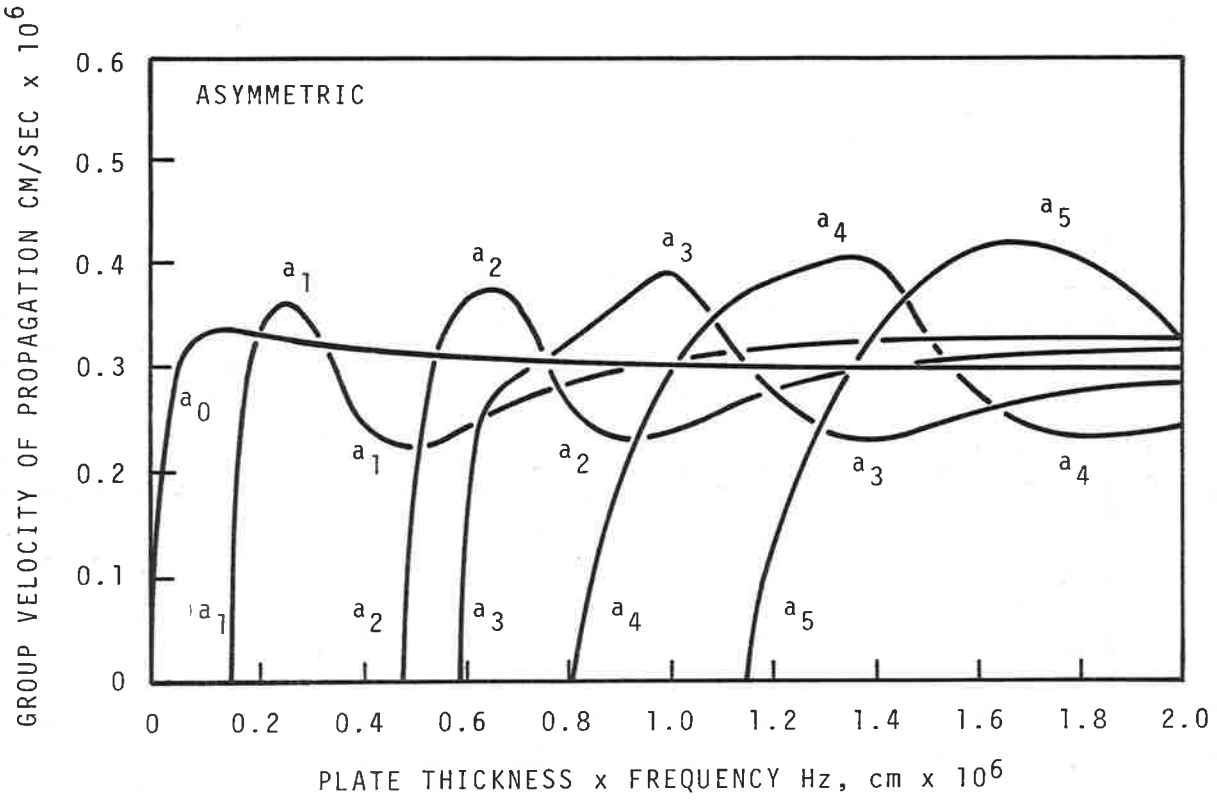

Figure 7. Group Velocities for Asymmetrical Lamb Modes in Steel

$$V_p = \frac{V_L}{\sin \theta} \qquad (1)$$

where V_L is the longitudinal velocity of the incident medium and θ is the incident angle measured from a line perpendicular to the plate surface. The incident phase velocity and the Fd product uniquely determine the particular Lamb mode which will be generated.

However, since we preferred to test the wheels from the tread surface, we used an edge excitation procedure. In this procedure, the ultrasonic waves are normally incident on the edge of the plate. When using this technique, it is no longer possible to control the phase velocity, and all allowable modes at a particular Fd product are generated. While it is possible to generate the several allowable modes, it has been observed[10] that the only modes containing appreciable energy are such that correspond to a relative maximum or minimum in the group velocity curves, at a particular Fd product. For this reason, only two or three principal modes are generated. The selection of a desired group of modes is attained by varying the frequency.

2.3 LAMB WAVE TEST PLATE DEFECT SENSITIVITY

Before proceeding with tests on full-size wheels, it was attempted to establish the basic sensitivity and optimum operating conditions, by using a flat test plate containing reference notches of various depths. The test plate was a flat, 1-inch thick steel plate, 10 x 28 inches long, with 1-inch long machined notches 0.05, 0.1, 0.2, 0.3, 0.4 and 0.5 inches deep. The notches were spaced on 4-inch centers, 4 inches from the long edge of the plate. A 0.1-inch deep notch positioned 14 inches from the 10-inch dimension also was included.

Optimum test frequencies in the test plate were established by varying the frequency over a 250 to 800-KHz range. The transducers used for these tests were driven with a 20 to 40-microsecond burst of sine waves. The response amplitude from the 0.1-inch deep notch, 6 inches from the plate edge, was compared to the longitudinal wave echo from the back surface of a 6-inch diameter test

block at each frequency. Optimum test frequencies were 300, 320, 350, 405, 450, 480, 575, 600, 740, and 760 Hz. These frequencies covered the Fd product range from 762 to 1930 KHz cm which included the third-through-the-sixth symmetric and asymmetric modes. Of these frequencies, the 450 and 760 KHz were the most sensitive.

The frequency dependence of the response from a 0.1-inch deep notch, 6 inches from the transducer, is shown in Figure 8. The incident energy at each frequency was normalized relative to the longitudinal wave echo from the back surface of a 6-inch diameter test block. The photographs in Figure 8 identify the responses from the 0.1-inch notch and the back surface.

The large signal at the left edge of each photograph is the initiating or main-bang pulse. The response at 450 KHz was approximately 5 percent greater than that at 440 or 460 KHz, but decreased rapidly above and below these frequencies.

Efficiency of mode generation for frequencies between 440 and 460 KHz is indicated by the amplitude of the back surface reflection in Figure 8. The group velocity of the propagated mode (0.5 x 10^6 cm/sec) most closely matches that of the S_3 mode at this Fd product (1140 KHz cm; see Figure 5). The 20-KHz bandwidth (440 to 460 KHz) shown in Figure 8 represents a span of 50.8 KHz cm or 4.4 percent. A thickness variation of 4.4 percent therefore would produce the same response variations as the 20 KHz frequency change shown in Figure 8. A swept frequency oscillator would be required to compensate for large thickness variations which would be encountered in testing full-size wheels.

Responses from 0.05 to 0.5-inches deep, 1-inch long notches are shown in Figure 9 for a test frequency of 760 KHz (1930 KHz cm). The group velocities of these response signals closely match the S_5 and A_6 modes at 1930 KHz cm (see Figures 6 and 7). Note that peak response signals from the smallest three notches occur later in time, while the larger two are composed of two superimposed signals. This results from a multi-mode propagation of the S_5 and A_6 waves. The slower A_6 wave appears to be more sensitive to small surface defects than the faster S_5 wave. Multi-mode propagation of this type may result in some confusion when estimating

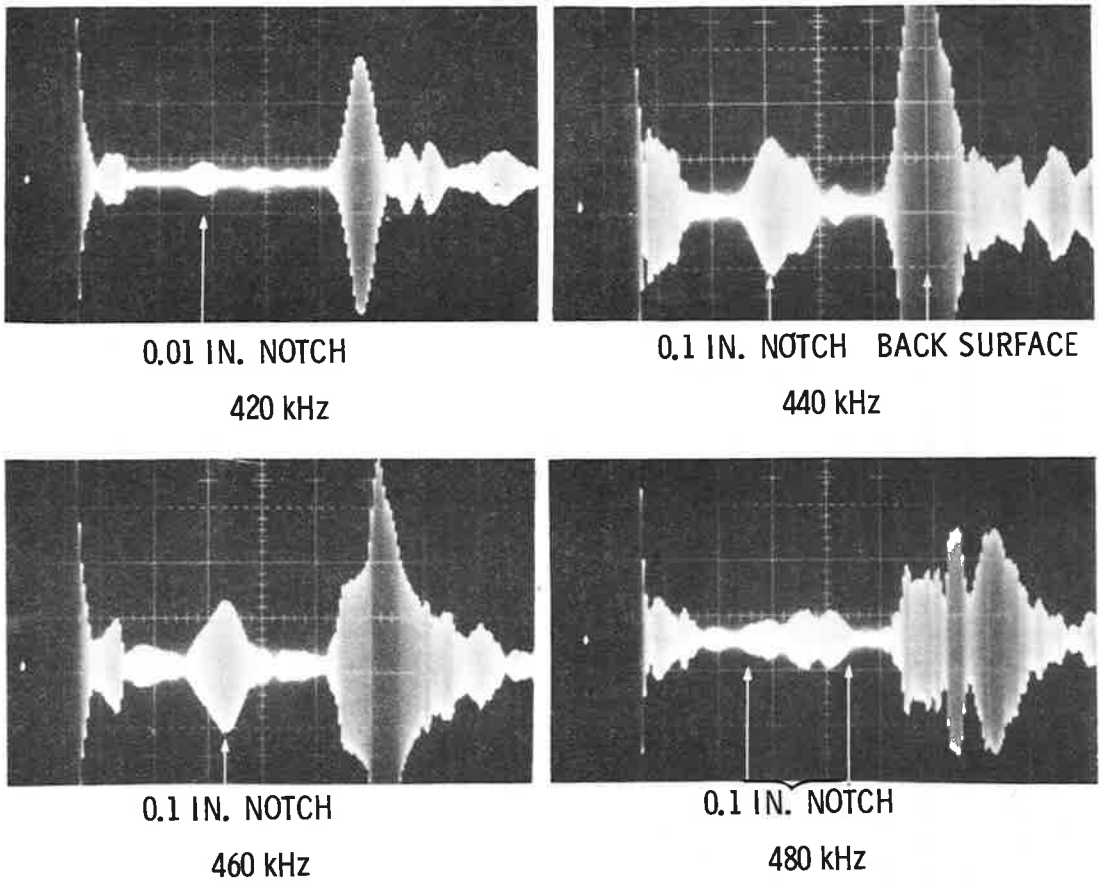

Figure 8. Lamb Wave Frequency Sensitivity for a 0.1-Inch Deep, 1-Inch Long Notch in a 1-Inch Thick Plate (Pulse Echo)

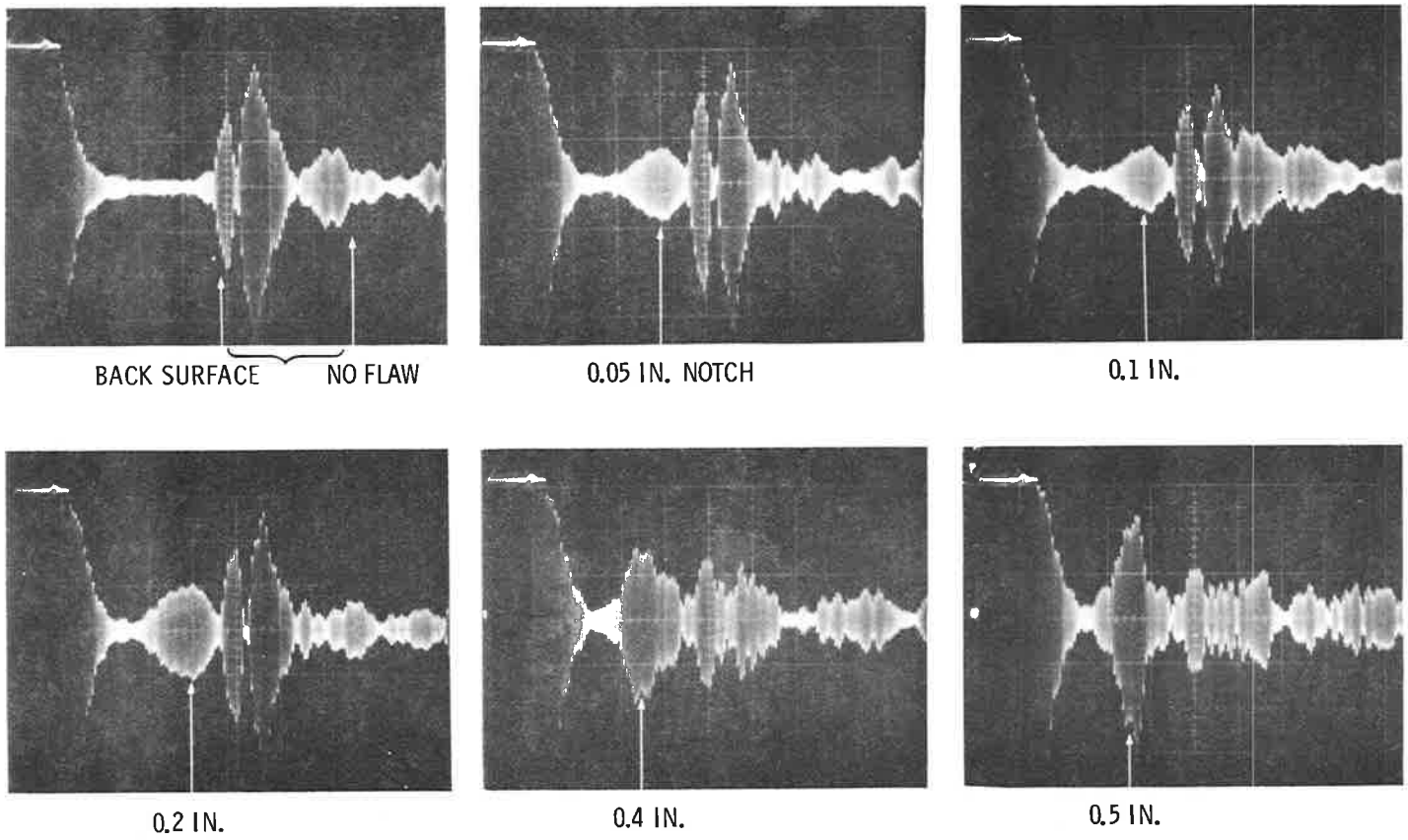

Figure 9. Lamb Mode Signal Responses from 0.05 to 0.5-Inch Deep, 1-Inch Long Notches in a 1-Inch Plate for a Test Frequency of 760 KHz (1930 KHz cm)

the location and number of defects present from the received signal. A plot of this signal is shown in Figure 10. This response was normalized to the response obtained from a back surface reflection at the same distance (6 inches). The solid line represents the area of the notch divided by 1 inch^2 (an assumed area for the back surface reflection). It can be seen from Figure 10 that the signal response is greater than could be expected if the signal amplitude depended directly on the flaw area alone. This would indicate that these Lamb waves are more sensitive to small surface flaws that to the same size defect located deeper in the plate. Similar results were obtained using a frequency of 450 KHz.

The generation of Lamb waves requires several cycles (25 or more for modes 3 and higher) of a particular frequency, before the plate mode condition can be efficiently established.[10] This can be understood from the fact that the number of allowed modes of propagation increases with increasing Fd product which makes it more difficult to generate a particular mode. The use of 25 cycles at 500 KHz, to generate a Lamb wave, would result in a dead time of 50 microseconds, which is equivalent to almost 6 inches of steel. This would mean that flaws closer than 6 inches from the transducer could not be detected, since they would be masked by the excitation signals. It is possible to use fewer excitation cycles; this would, however, significantly reduce the signal amplitude of the generated mode.

2.4 LONGITUDINAL-SHEAR WAVE TECHNIQUE

The Pulse-Echo Longitudinal-Shear technique uses a short burst (2 to 5 cycles) of high-frequency (1 to 3 MHz) sound waves. This reduces the long near-surface dead time encountered in the Lamb wave method. The shock pulse excitation, common to most general-purpose ultrasonic instruments, provides an exponentially decaying sine wave burst. The frequency and number of cycles in the burst are basically determined by the pulser waveform, resonant frequency, and damping characteristics of the tranducer. For Fd products larger than about 800 KHz cm, this type of pulse will

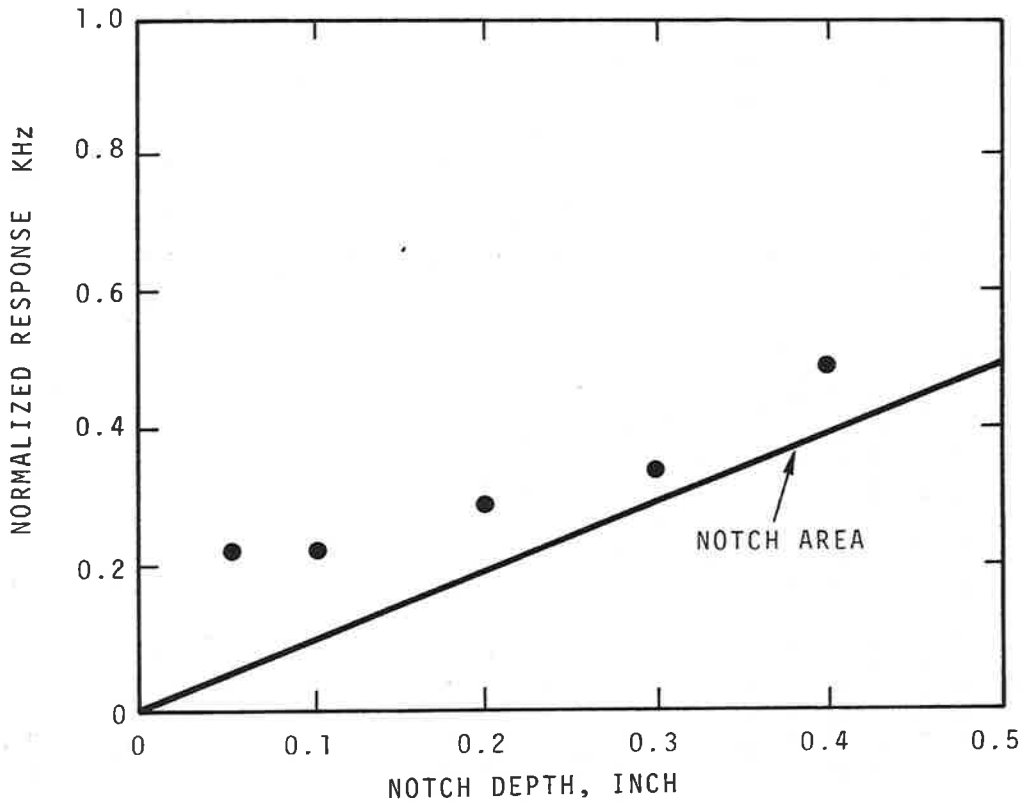

NOTES:

1. Solid line represents the ratio of notch area to 1 sq. in.
2. Test frequency = 760 KHz.
3. FXd product = 1930 KHz cm.

Figure 10. Lamb Wave Response Amplitude from 1-Inch-Long Test Plate Notches Normalized to Total Reflection from a Back Surface at the Same Distance (6 Inches)

not significantly excite Lamb waves. The propagation will conform more closely to that shown in Figure 11.

Propagation in the plate, as shown by Figure 11, results from reflections and shear mode conversions of the diverging longitudinal wave generated at the plate edge. Longitudinal waves striking the surface of a steel plate at grazing incidence (greater than 70°) cause a portion of the energy to be mode-converted to shear waves, at an angle of 33° from a line perpendicular to the plate surface.[14] A portion of this shear wave is, in turn, mode-converted back to a longitudinal wave, at each reflection. After a short distance, the incident pulse is partitioned into longitudinal waves predominently parallel to the plate surface and shear waves at 33°. Figure 12 shows typical signals received by the transducer for a back surface reflection at 10 inches. The first signal is the direct longitudinal wave. Each of the following multiples represents 1, 2, 3, etc., shear-wave paths. The spacing between multiples is determined by the plate thickness and the longitudinal-to-shear velocity ratio. An approximate formula for this spacing(s) can be written as:

$$s = d\sqrt{\left(\frac{V_L}{V_t}\right)^2 - 1} \qquad (2)$$

where d is the thickness of the plate, V_L and V_t are the longitudinal and shear velocities. For our test plate, the calculated spacing was 0.77d, and the measured value of 0.78d.

2.5 LONGITUDINAL-SHEAR TEST PLATE DEFECT SENSITIVITY

The sensitivity of the Longitudinal-Shear Wave technique was demonstrated on the flat-plate standard, using an Automation Industries UM 771 Reflectoscope and a 2 MHz, 1-inch diameter transducer. Signal responses from the 0.05, 0.1 and 0.2-inch deep notches in the test plate are shown in Figure 13. The transducer was applied at the edge of the plate with the notches 6 inches from the front surface and 4 inches from the back surface. Note the relative amplitude for the various paths, as compared to the distribution, shown in Figure 12. The direct longitudinal reflection

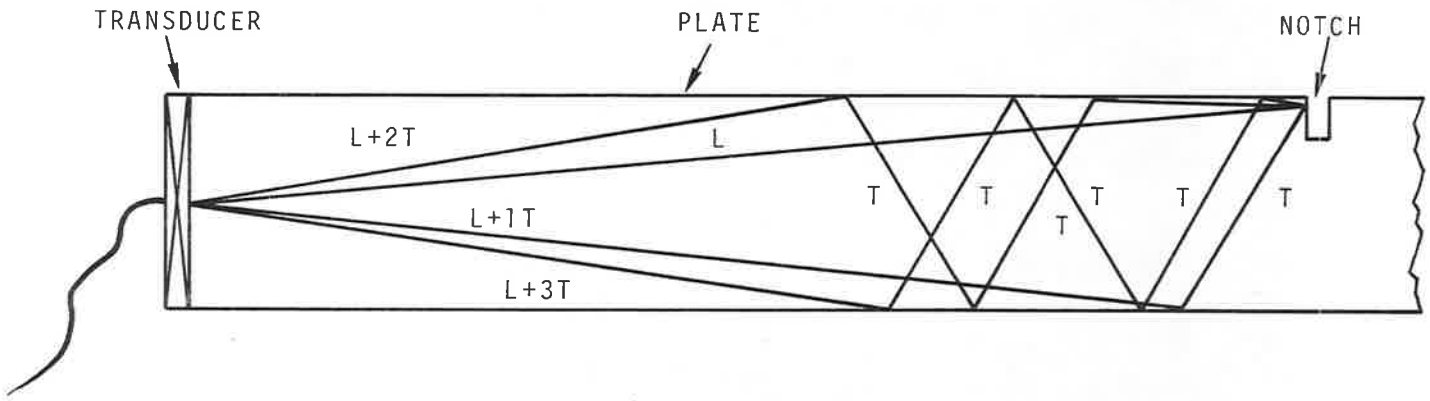

Figure 11. Mode Conversion and Multiple Path Propagation in a Plate, Showing the Possible Paths for Direct Longitudinal (L) and 1, 2, and 3 Shear-Mode Multiples (L + 1, 2, or 3 T)

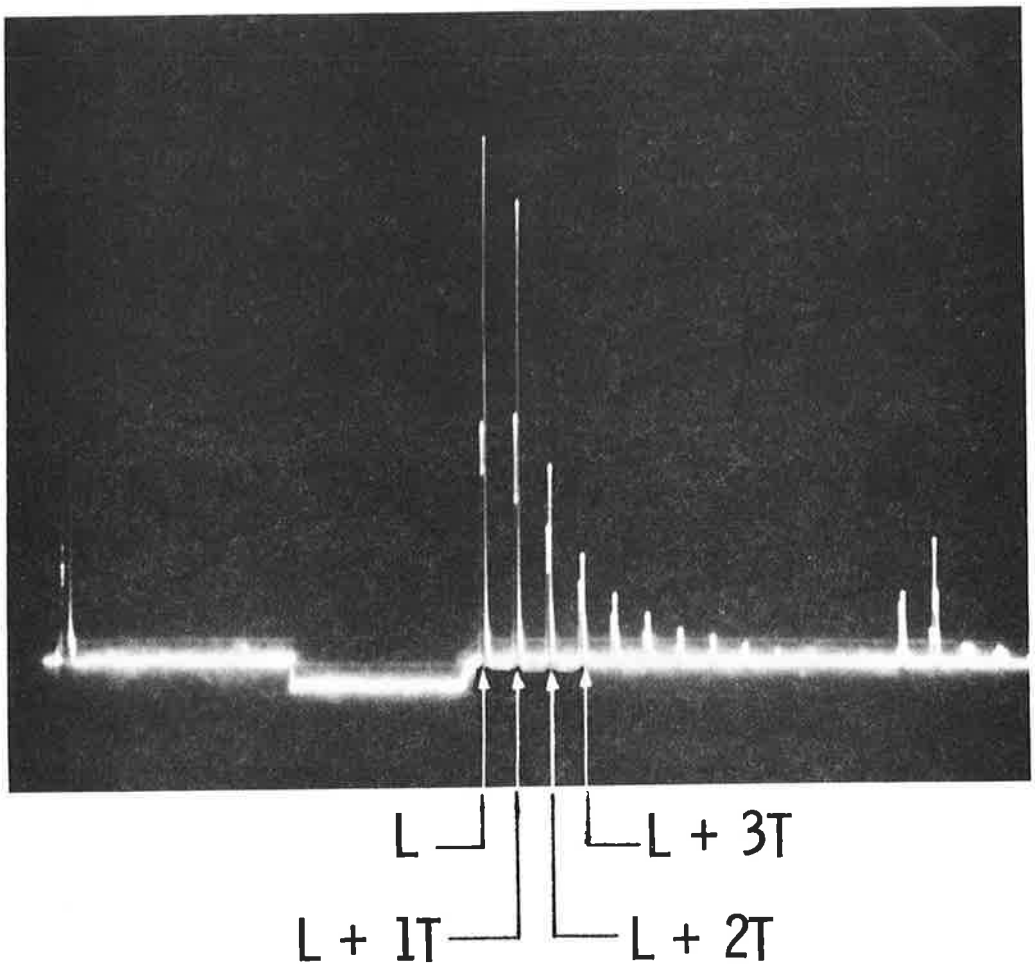

Figure 12. Typical Plate Pulse Echo Signals (Back-Surface Reflection at 10 Inches in a 1-Inch Plate)

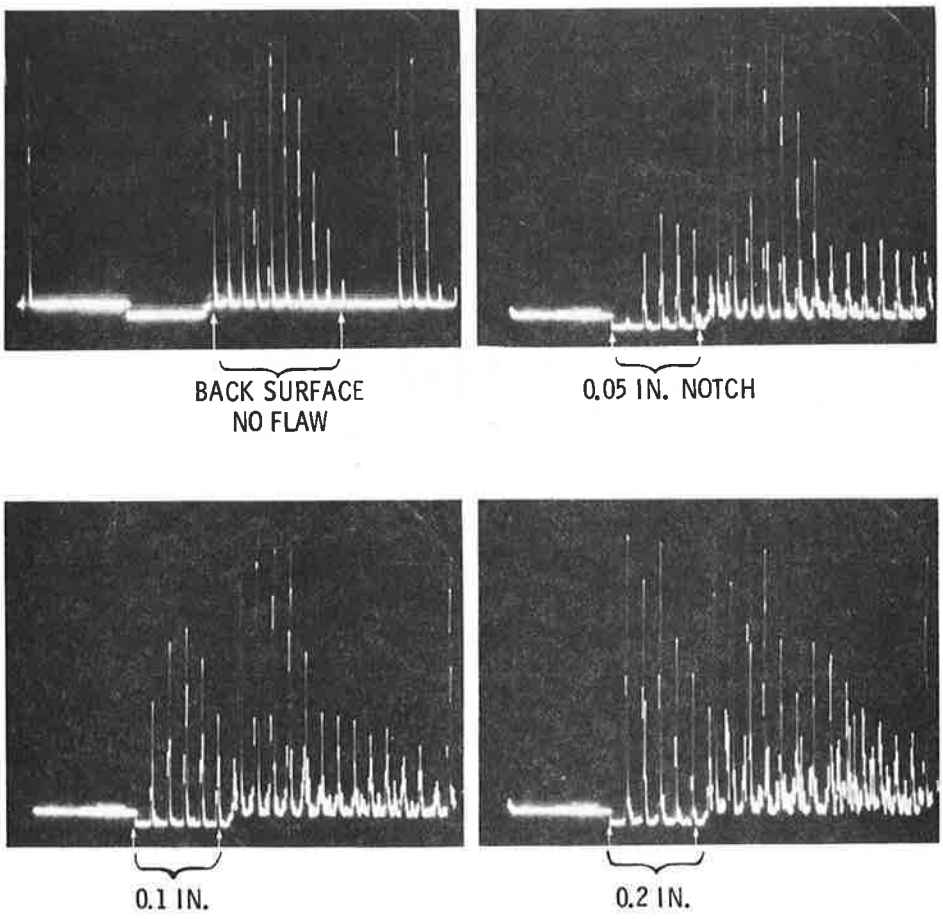

Figure 13. Longitudinal-Shear Signal Response from 0.05, 0.1, and 0.2-Inch Deep, 1-Inch Long Notches in the Standard Test Plate, Test Frequency 2 MHz

(first signal within the gated region) is barely detectable for the 0.05-inch notch, but increases rapidly with flaw size. This indicates that the shear waves are more sensitive to small flaws than are longitudinal waves.

Flaw sensitivity is shown graphically in Figure 14. The response from each flaw was normalized to a back surface reflection at 6 inches. The solid line labeled in Figure 14 is the area of the notch divided by 1 $inch^2$, while the dashed line represents linear nature of the response for the three smallest flaws. The deviation of the response from the notch area line results from a partition of energy into the various modes and the ratio of notch size to wavelength. The apparent lower sensitivity of this test, as compared to the Lamb wave technique shown in Figure 10, is more than offset by the improved signal-to-noise ratio.

The hub flaws to be detected can be located as far as 14 inches from the tread surface, depending on wheel size. It is necessary to know the sensitivity over this range. Figure 15 depicts the relative amplitude of responses from 0.1-inch deep notches at 6 and 14 inches from the transducer. The response at 14 inches is approximately half that at 6 inches. The use of distance amplitude correction (DAC) could be applied to normalize the response over the required range, as the signal-to-noise ratio even at 14 inches is still very good.

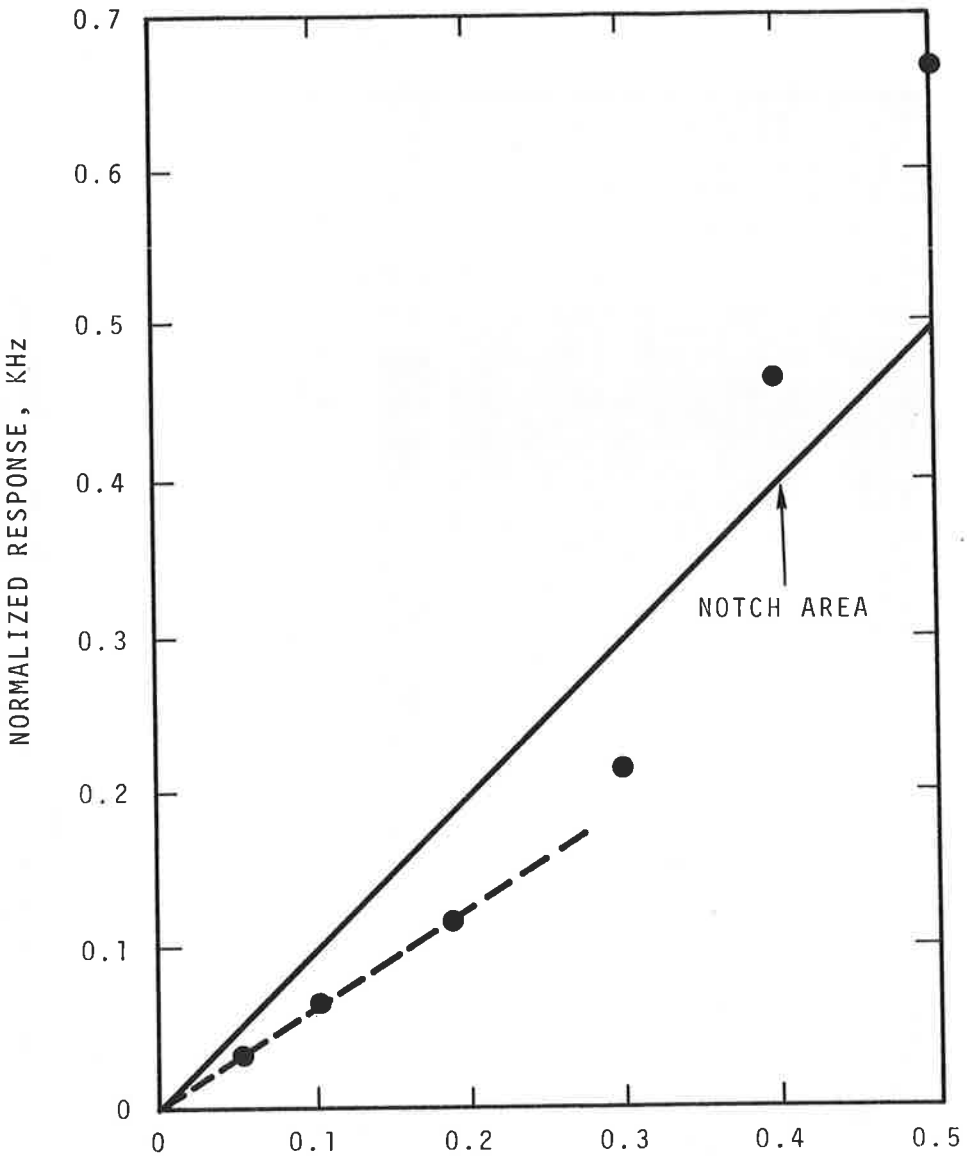

NOTES:

1. Response normalized to back surface reflection at the same distance as notch (6 inches).
2. Dashed line indicates the linear nature of responses from 0.05, 0.1 and 0.2-inch deep notches.
3. Solid line represents the ratio of notch area to 1 square inch.

Figure 14. Normalized 2-MHz Pulse Echo Response from Standard Test Plate Notches

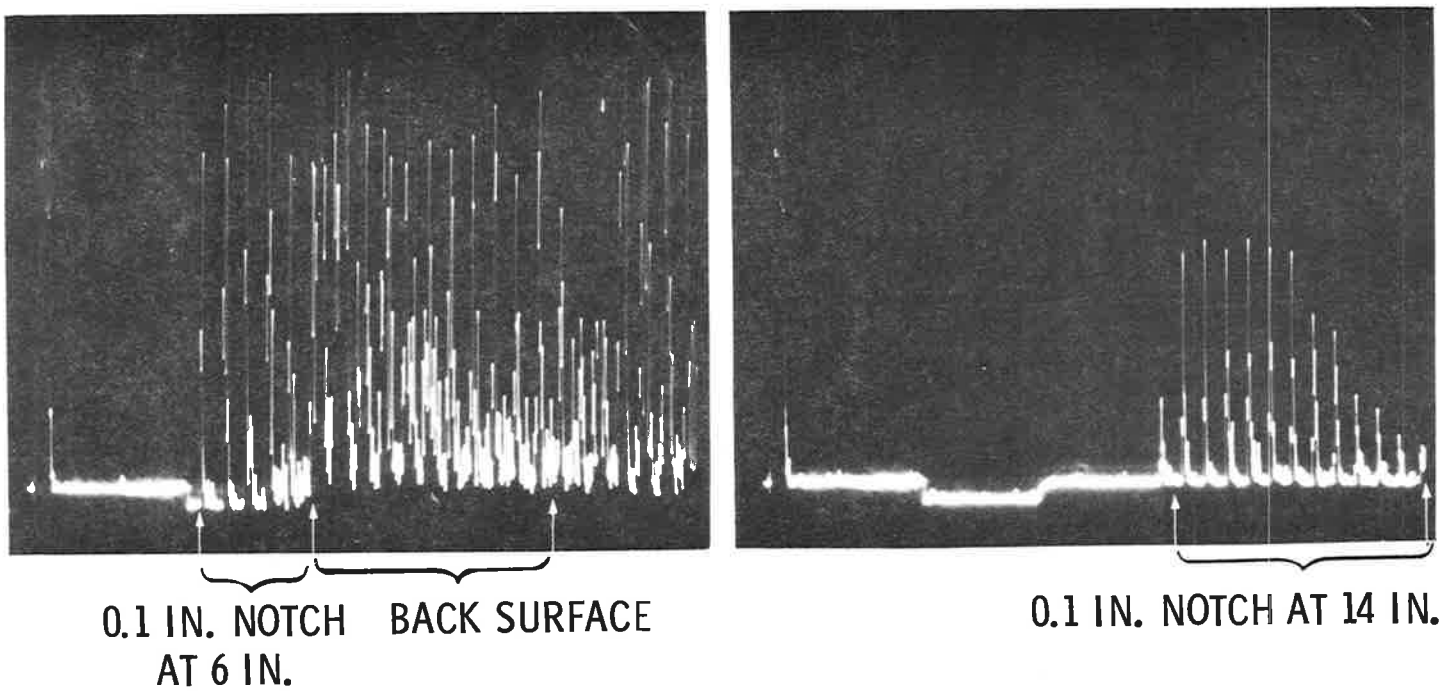

Figure 15. Longitudinal-Shear Response from 0.1-Inch Deep, 1-Inch Long Notches in the Standard Test Plate at Ranges of 6 and 14 Inches, Test Frequency 2 MHz

3. WHEEL INSPECTION

3.1 DESCRIPTION OF APPROACH

In applying these test procedures on full-size railroad wheels, the effort faced two specialized problems not encountered with the flat test plate. The first and most obvious difference to be considered was the cylindrical shape of the tread surface. The second was the shape of the rim and the rim-to plate transition. Divergence of the sound beam in the rim area can result in multiple undesirable reflections within the rim. These reverberations not only yield false indications, but they may mask the presence of an actual flaw and reduce the total energy transmitted down the plate.

The cylindrical nature of the tread surface was accommodated through the use of a specialized transducer wear face that was ground to match the circumference of the wheel. A detailed discussion of the transducers used in these tests, as well as a recommended design for further development, is contained in Appendix A. The curvature of the wear face does not necessarily have to be exactly that of the wheel. In fact, a transducer designed to fit a 33-inch wheel performed as well on 28 and 36-inch wheels, as transducers specifically designed for the respective sizes.

Rim reverberations presented a more serious problem; a typical rim reverberation path is shown in Figure 16. The obvious solution is to utilize a small, collimated ultrasonic beam. This, however, is not easily accomplished. The divergence angle (ϕ) of an ultrasonic beam,[15] is given by

$$\sin \phi = 1.22 \frac{\lambda}{2r} \qquad (3)$$

where λ is the wavelength in the material, r is the radius of the transducer, and ϕ is the $\frac{1}{2}$ angle of the divergence measured from the beam centerline. Wheel plate thickness limits the maximum transducer size, since it is preferred that this beam be smaller than the plate thickness.

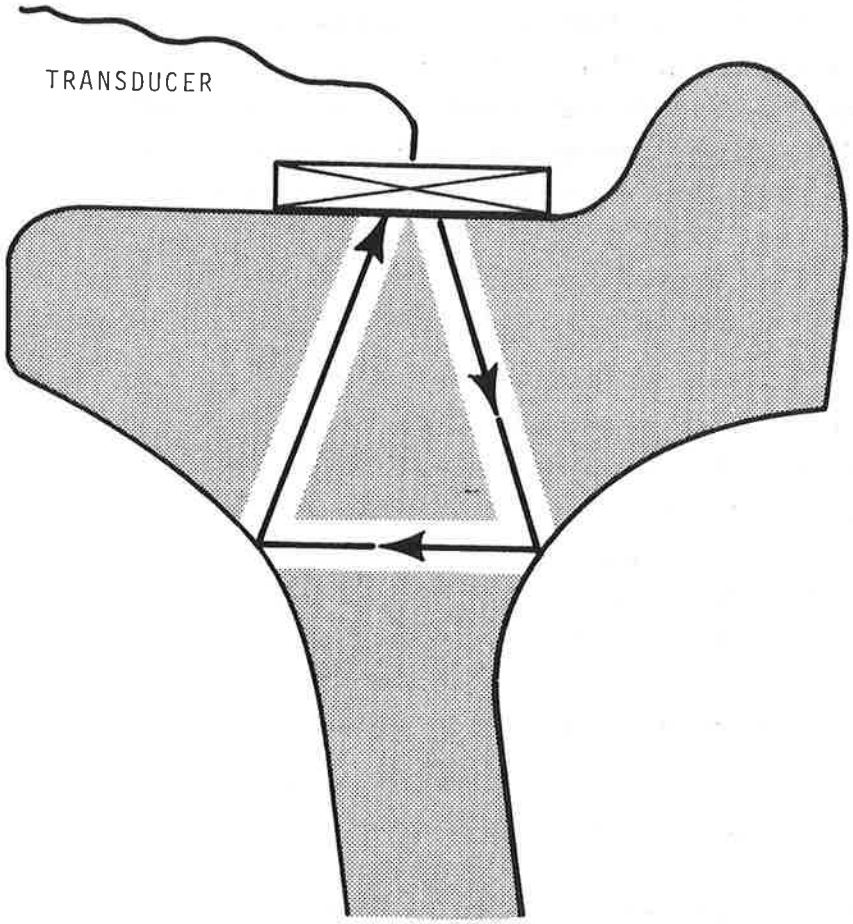

Figure 16. Typical Rim Reverberation Propagation Paths

The minimum wavelength or maximum frequency is limited by the attenuation and path length. In addition, in Lamb wave testing, the frequency is further limited by the Fd product of the desired mode. Therefore, the best compromise had to be selected to achieve a minimum of spurious rim reverberations. (The word spurious in this report is used to indicate signals arising from sources other than defects or simulated defects.)

In addition to transducer size and frequency, acceptance gates and optimum transducer positioning were used to reduce the influence of spurious signals. Since most wheel-plate, service-induced cracks are principally circumferential and confined to the areas where the front hub and rear rim fillets merge with the plate, inspection efforts could be concentrated on these areas. Electronic acceptance gates positioned in the appropriate areas greatly reduced the influence of spurious signals. Optimum positioning of the transducer also was used to achieve maximum sound transmission down the plate.

3.2 STANDARD TEST WHEELS

It was intended to obtain a representative selection of full-sized wheels with service-induced defects. Most wheel failures being currently detected by visual inspection, the choice was limited almost entirely to very large flaws. Therefore, new and used wheels with machined, reference test notches were selected; the radial location of the notches is shown in Figure 17. The notches were angularly separated about the wheel axis by a minimum of 45 degrees. In each case, the notch was located at the point where the front hub or the rear rim fillet merged with the plate. The notches were identified as FFN2 and BFN1, respectively (see Figure 17). The reference notches were 1.5 long, 0.25 inches wide and either 0.125 or 0.25 inches deep. The sides of the notches were milled perpendicular to the plate surface, and the 1.5-inch dimension of each notch was perpendicular to the wheel radius. Wheels obtained for this evaluation included types B-28, J-33, H-36 1-wear, and M-33 2-wear, straight-plate wrought, and a CJ-33 parabolic-plate cast wheel; all but the CJ-33 were used wheels.

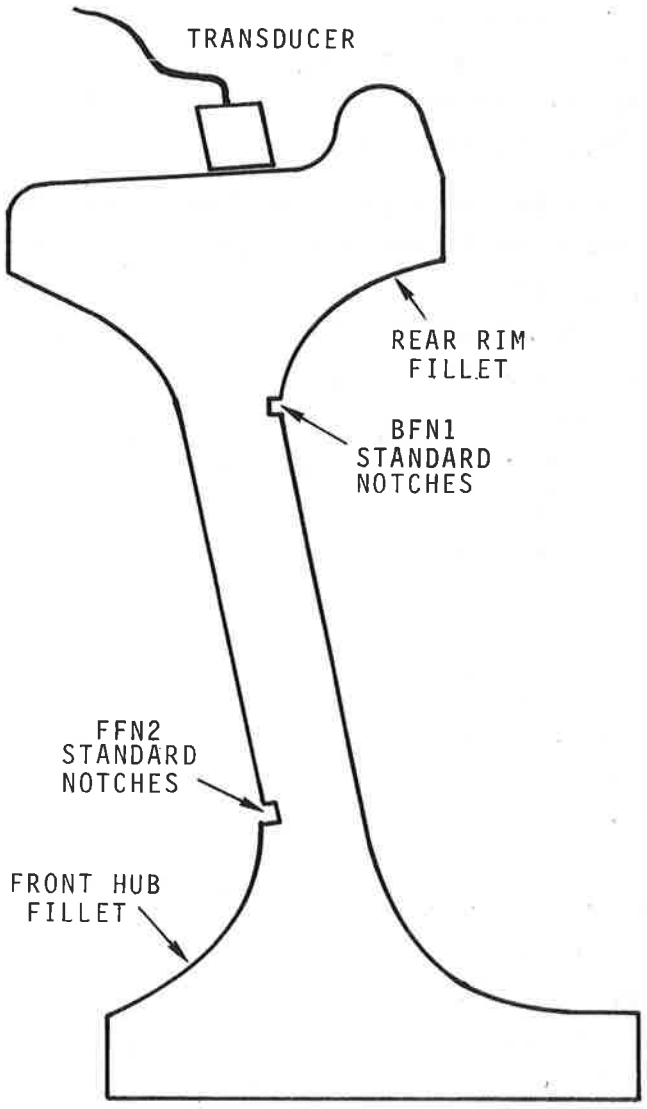

NOTE:

All the notches are angularly separated by a minimum of 45°.

Figure 17. Radial Location of Standard Notches in Full-Size Wheels

3.3 LAMB WAVE TESTING

This paragraph reports the results obtained from Lamb wave testing on wheels with $\frac{1}{4}$ and $\frac{1}{8}$-inch deep notches. Lamb wave testing was accomplished only on the J-33 and H-36 wheels, because the technique was dropped early in the program before the remaining wheels were received, in favor of the Longitudinal-Shear technique.

Optimum test results were obtained on the H-36 wheel, at a frequency of 640 KHz (see Figure 18). The transducer was driven by a 20-microsecond-long sine wave burst resulting in a dead time of approximately 30 microseconds, due to transducer ring down. A longer drive pulse yielded larger Lamb mode reflections from the hub flaws, which however, totally obscured the rim BFN1 defects. Even at this setting, the length of the drive pulse partially interferred with the BFN1 notch responses. This interference became readily apparent when the drive pulse was shortened and the notch responses peaked approximately 10 microseconds earlier in time, with a slightly higher amplitude. It should be noted here that the responses from BFN1 notches were longitudinal waves rather than Lamb waves, because Lamb waves were not generated until the incident longitudinal wave had propagated 1 to 2 inches down the plate. The transducer used for these tests was a 600-KHz 1.5 long by 1-inch wide unit with the element ground to fit the curvature of a 33-inch diameter wheel; the long dimension of the transducer being oriented in the circumferential direction.

In Figure 18, the hub FFN2 responses for the $\frac{1}{4}$ and $\frac{1}{8}$-inch deep notches appear to be S_4 and A_5 Lamb modes, as determined from the velocity of propagation and an average Fd product of approximately 1500 KHz cm. The signals which occur between the main-bang and the notch signals result from rim reverberations. Minimum signal-to-noise ratios for the detection of $\frac{1}{8}$-inch notches are from 2 to 3. Similar results were obtained on the J-33 wheel at an optimum frequency of 620 KHz, with the exception that slightly lower signal-to-noise ratios were obtained.

In an attempt to reduce the influence of the spurious rim reverberations, the two transducer pitch-catch technique was

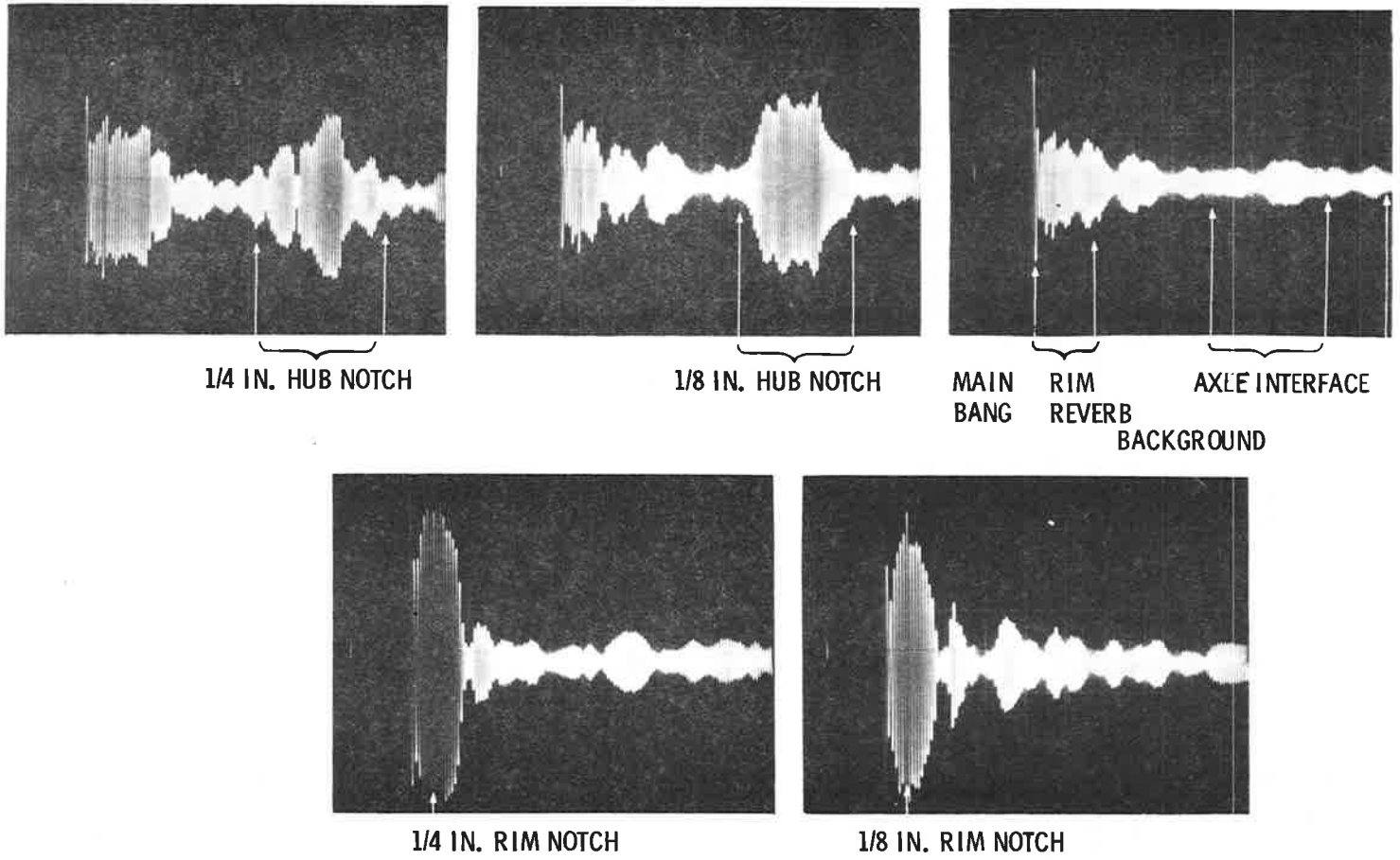

Figure 18. Lamb Wave Signal and Background Response from 1/4 and 1/8-Inch Deep FFN2 Hub and BFN1 Rim Notches in the H-36 Wheel for a Test Frequency of 640 KHz

employed. In this method, a separate receiver was placed on the tread approximately 0.5 inches (circumferentially) from the transmitting transducer. The receiver was similar in design to the transmitter except smaller (1 inch long by 0.5 wide). The results of this test are shown in Figure 19 for the J-33 wheel at 620 KHz. The Fd product at this frequency and a plate thickness 0.75 inches or 1.9 cm would indicate an S_3 Lamb mode. The group velocities of these signals closely approach that of the S_3 Lamb mode at 1180 KHz cm. The lower trace in Figure 19 is the response of the receiving transducer on the tread surface. The upper trace is the response of an electromagnetic acoustic (EMAC) transducer on the plate surface directly in front of and adjacent to the FFN2 notch; the EMAC transducer is described in Appendix B. Note that these are signal-mode signals, one principal peak, as compared to multimode signals in Figure 18. The upper trace indicates the nature of the energy incident on and directly reflected from the notch. The signal-to-noise ratio for a $\frac{1}{8}$-inch FFN2 notch is, again, approximately 2.

The pitch-catch technique did eliminate near-surface dead time and substantially reduced the influence of rim reverberations. However, the signal-to-noise ratio in the area where notch signals were received was not substantially improved. Response to rim notches, however, was drastically reduced in this configuration, due to the relatively large included angle between the transducers for a near-surface flaw. The single transducer technique is still the most feasible method for the detection of rim flaws.

3.4 LONGITUDINAL-SHEAR WAVE TESTING

Application of the Longitudinal-Shear method to full-size wheels is described below. This technique is particularly advantageous for the detection of BFN1 rim fillet defects, due to its relatively short near-surface dead time and the improved resolving power of the higher test frequencies. Ultrasonic waves incident at BFN1 defects are purely longitudinal, for both test techniques, as Lamb waves are not generated until the energy enters the plate area of the wheel. Therefore, there is no reason why a long burst of lower frequency sound should be used for the detection of rim

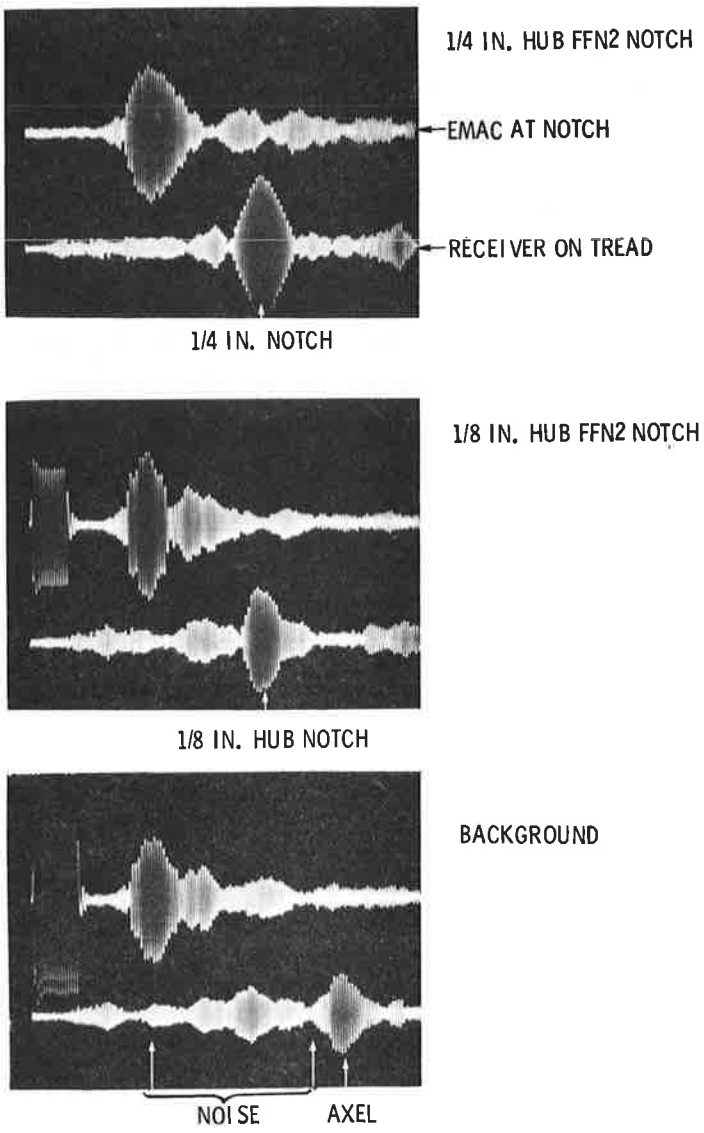

NOTES:

1. Upper trace is the response of the EMAC transducer adjacent to the notch.

2. Lower trace is the response from the receiving transducer on the tread adjacent to the transmitter.

Figure 19. Two-Transducer, Pitch-Catch Response from 1/4 and 1/8-Inch Deep FFN2 Hub Flaws in the J-33 Wheel for a Test Frequency of 620 KHz

defects. Short bursts of frequencies between 1 and 3 MHz are much more suitable.

The initial effort consisted of determination of optimum test parameters, i.e., frequency, transducer design, and transducer position on the tread surface for each wheel. In the development of optimum test procedures, transducers (described in Appendix A) of several sizes, types, and frequencies were evaluated. Of these, the most suitable configuration was found to consist of units 0.5 wide and 1 inch long, with a bonded wear-face ground to match the wheel curvature. These units were the most efficient type for coupling sound reliably into the wheel. The narrow width of the transducers allows a better fit of the wear face to the profile of the worn tread surface. Frequencies from 1 to 3 MHz were also evaluated. Figure 20 compares the relative background for test frequencies of 1 and 3 MHz with gain adjusted to give approximately equal response for $\frac{1}{4}$-inch hub flaws on the J-33 wheel. The 1-MHz signal has a slightly better signal-to-noise ratio. The 1-MHz transducer also has the advantage of being somewhat less sensitive to couplant variations.

Responses from BFN1 flaws were, in general, approximately ten times greater than from FFN2 flaws, this resulting from the shorter path length and the lack of energy partitioning due to mode conversions which occur in plate propagation. For FFN2 flaw detection, the optimum transducer position on the tread surface for all wheels (except the CJ-33 parabolic plate wheel) was 2.85 inches from the front face of the rim. For detection BFN1 rim flaws, the optimum transducer position was approximately 0.2 inches closer to the back of the wheel. The configuration of the CJ-33 parabolic plate wheel required the transducer to be placed as closely as possible to the flange.

A compromise test procedure was developed which was applicable to the straight plate wheels (B-28, J-33, H-36 and M-33). In this test, the transducer is placed on the tread 2.85 inches from the front face of the rim for the detection of hub flaws, and 3.02 inches from the front face, for the detection of rim flaws. Responses from reference notches in the test wheels using this test

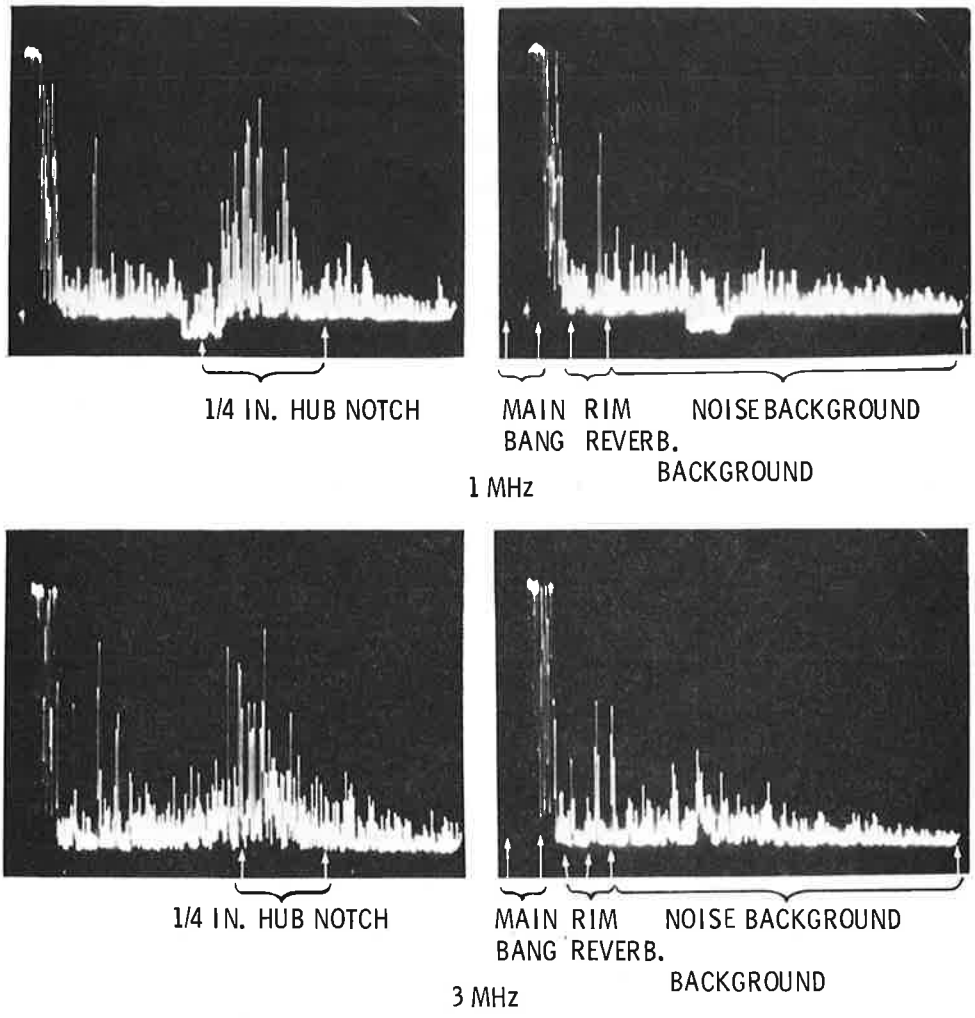

Figure 20. Relative Longitudinal-Shear Signal and Background Responses for Test Frequencies of 1 and 3 MHz from 1/4-Inch Deep FFN2 Hub Notches in the J-33 Wheel

procedure are shown in Figures 21 through 24. These tests were all performed using identical frequency and gain settings so that the relative signal amplitude for each wheel could be compared.

Baseline clipping or reject of approximately 0.5 cm was used to limit baseline noise. The 1-MHz transducer previously described was used for each wheel. The electronic acceptance gates were adjusted to accept indications from depths corresponding to the rim and hub fillets and included enough range to allow for the various wheel sizes. The gain settings for rim flaws constituted a factor of ten less than that used for hub flaws.

It is apparent from Figures 21 through 24 that defects located in the BFN1 rim fillet area should pose no problems, since they are easily detectable and are well above any noise level. On the other hand, flaws in the FFN2 hub fillet area must be separated from the background by using the acceptance gates. The spurious signals shown in the photographs result from rim reverberations which generally will not interfere with signals from BFN1 or FFN2 flaws, since they fall between the two signals. In Figure 22 (the J-33 wheel), there are also some extraneous signals (labeled "Rough Plate Area") which result from extremely rough profile machining of the plate. In general, responses to $\frac{1}{4}$-inch flaws are larger in amplitude and contain a greater number of multiples than $\frac{1}{8}$-inch flaws. Also, notice the differences in multiple spacing between the thinnest plate (0.8 inches for the B-28, Figure 21) and the thickest plate (1.1 inch for the H-36, Figure 23). We see no evidence of reflections from the hub-to-axle interface in Figures 21 through 24. One reason for this is that there was very little acoustic impedance difference between the wheel and axle material, resulting in little, if any, signal being reflected at the interface. The white lead compound used during wheel mounting also helped to couple the sound from the hub to the axle by filling the small voids which were normally present. The second, more important reason is that the plane of the plate was not normal to the axle and longitudinal waves from the plate were reflected at an angle which trapped much of the sonic energy in the hub. Likewise, shear waves would also be almost totally trapped in the hub due to

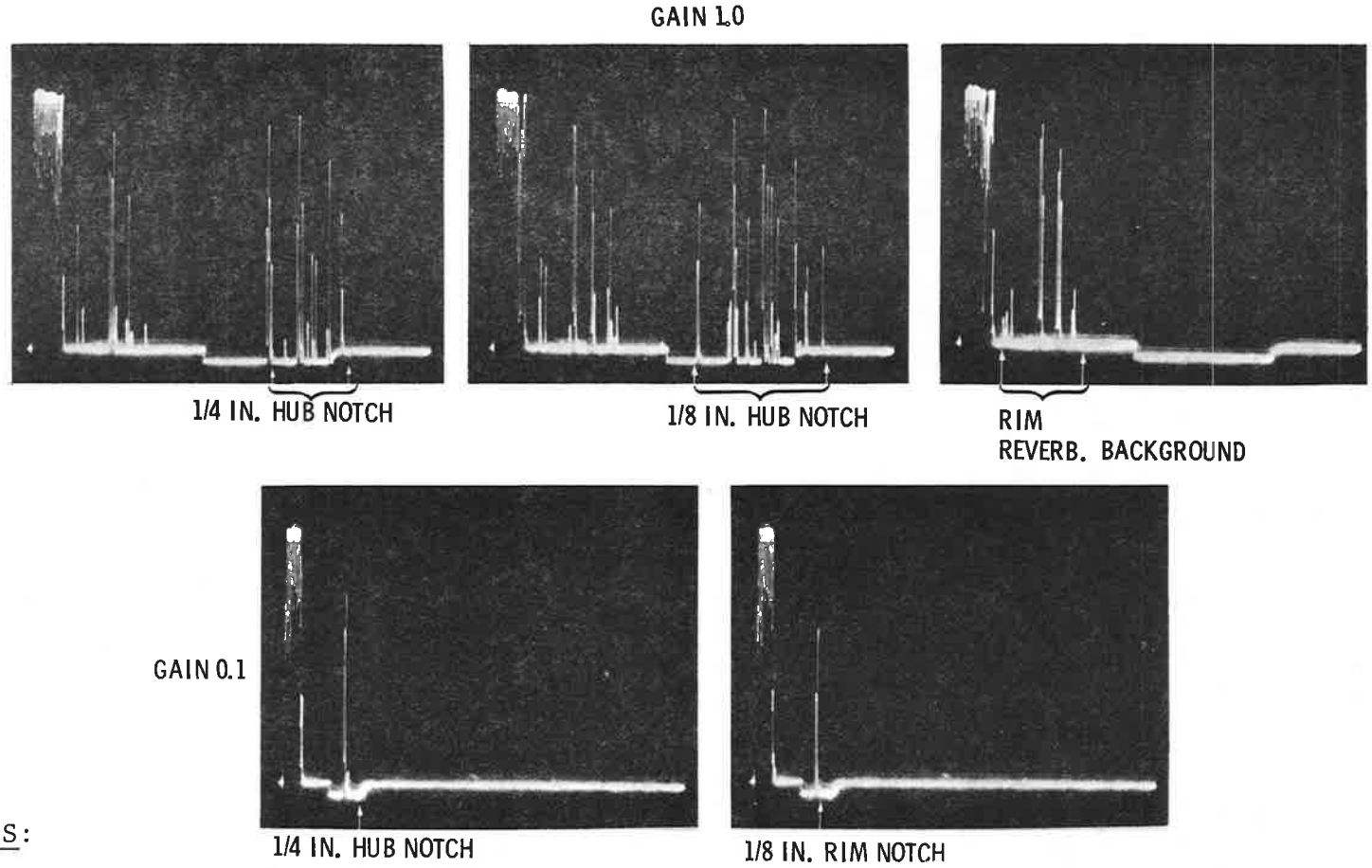

NOTES:

1. The gain for BFN2 rim flaws is approximately 1/10 of that used for FFN2 hub flaws and background response.
2. Test frequency = 1 MHz.

Figure 21. Longitudinal-Shear Signal Response from Standard Notches in the B-28 Wheel, Using the Compromise Test Procedure in which Frequency, Gain, and Transducer Position for Each of the Straight Plate Wheels is Held Constant

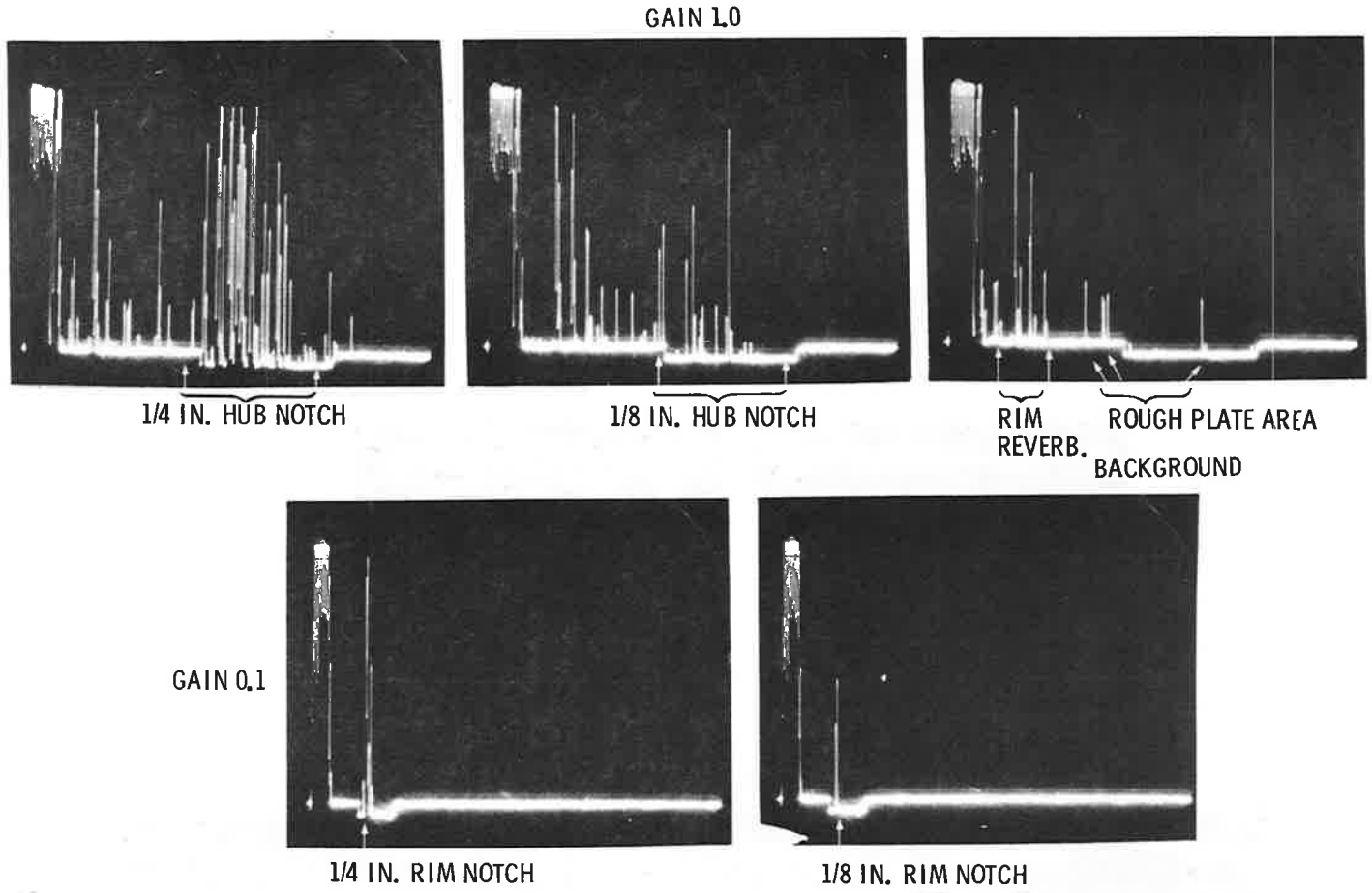

NOTE:

See Notes in Figure 21.

Figure 22. Longitudinal-Shear Signal Response from Standard Notches in the J-33 Wheel, Using the Compromise Test Procedure in which Frequency, Gain, and Transducer Position for Each of the Straight Plate Wheels is Held Constant

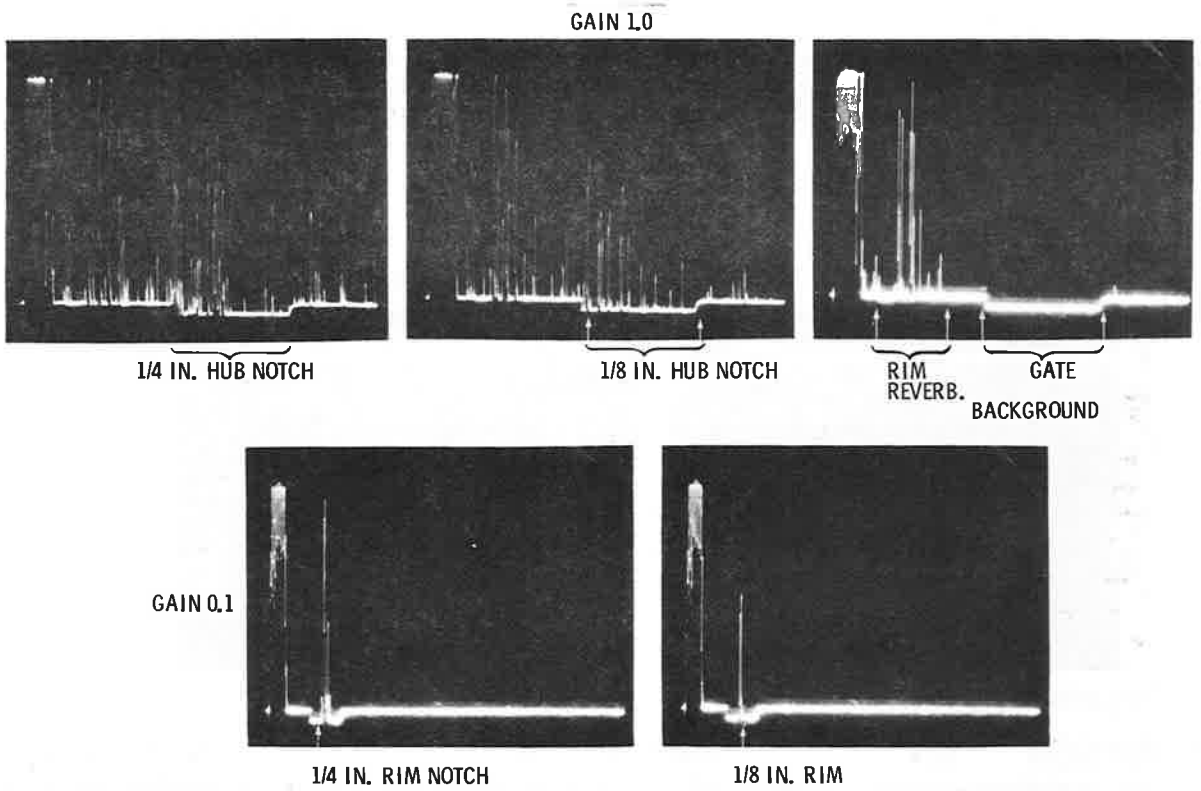

NOTE:

See Notes in Figure 21.

Figure 23. Longitudinal-Shear Signal Response from Standard Notches in the H-36 Wheel, Using the Compromise Test Procedure in which Frequency, Gain, and Transducer Position for Each of the Straight Plate Wheels is Held Constant

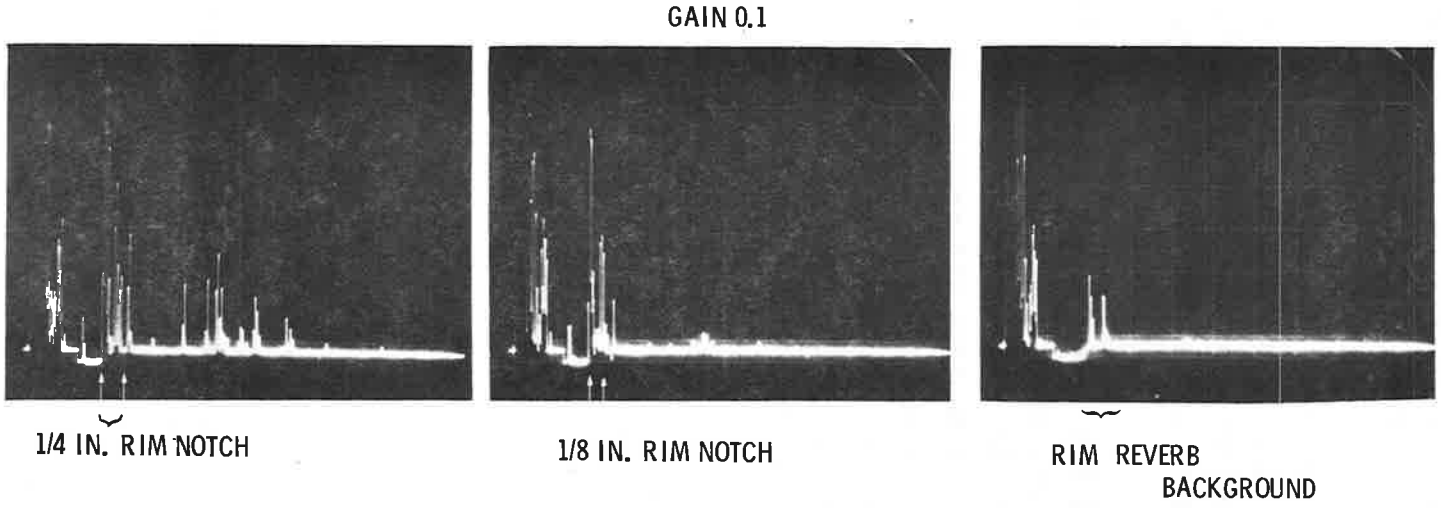

Figure 24. Rim Response in the M-33 Wheel, Using the Compromise Test Procedure in which Frequency, Gain and Transducer Position for Each of the Straight Plate Wheels is Held Constant

their zigzag propagation path. Even when no axle was present (as in the case of the B-28 wheel), very little signal was received from the hub bore interface at this gain setting. This is an extremely advantageous condition, since the flaw multiples would overlap the axle interface signal and would complicate detection and interpretation. This condition also allows the use of a wide acceptance gate, to accommodate all of the wheel sizes with only one gate setting.

Responses from the FFN2 hub flaws in the 2-wear M-33 wheel have been omitted from the previous discussion, because they were not adequately detectable at the reference gain setting used for the tests described. Figure 25 depicts the response for this wheel. The transducer was positioned directly over the $\frac{1}{4}$-inch FFN2 flaw, and the gain settings were exactly the same as used for the 1-MHz condition shown in Figure 20. The gain had to be increased by approximately 50 percent before the flaw signals (shown in Figure 26) could be detected; this resulted in the high noise level shown. The gate was positioned to include only the first flaw indications and to exclude hub bore signals (axle not installed). The installation of an axle would slightly improve this condition. However, the large rim reverberation signals are not well separated from the gated area, increasing the probability of false flaw indications.

It is difficult to establish specific reasons for the lack of sensitivity to FFN2 flaws on this 2-wear M-33 wheel. It is not a problem of material attenuation, since this wheel (when measured through the rim or plate) exhibited a slightly lower attenuation than the J-33 wheel. The only apparent reasons appear to be the thickness of the rim and the shape of the rim-to-plate transition. Evidently, rim reverberations and increased scattering in the plane of the wheel substantially reduces the total energy incident at the flaw.

Results of a slightly better test for FFN2 flaws in the 2-wear M-33 wheel are shown in Figure 27. The transducer used in this test was larger, measuring 1.0-inch wide by 2.0-inches long, as compared to the 0.5 by 1.0-inch transducer used for the tests shown

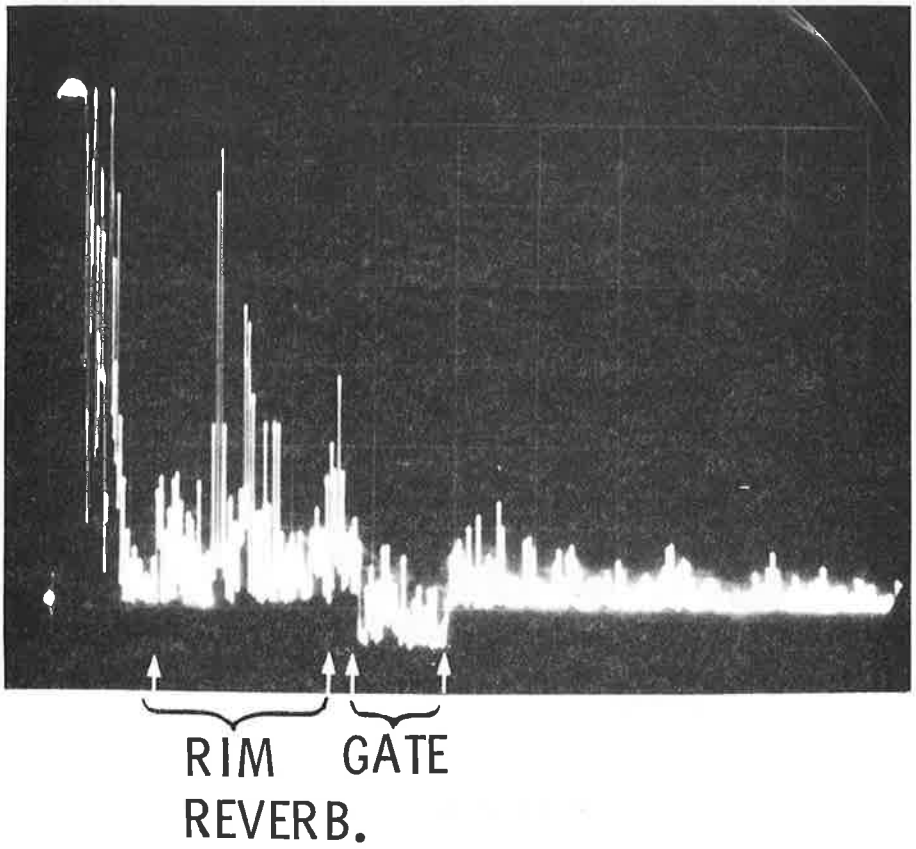

NOTE:

Notch response is not detectable at this gain setting.

Figure 25. Relative Longitudinal-Shear Signal and Background Response for Test Frequencies of 1 and 3 MHz and from 1/4-Inch FFN2 Hub Flaw in the M-33 Wheel

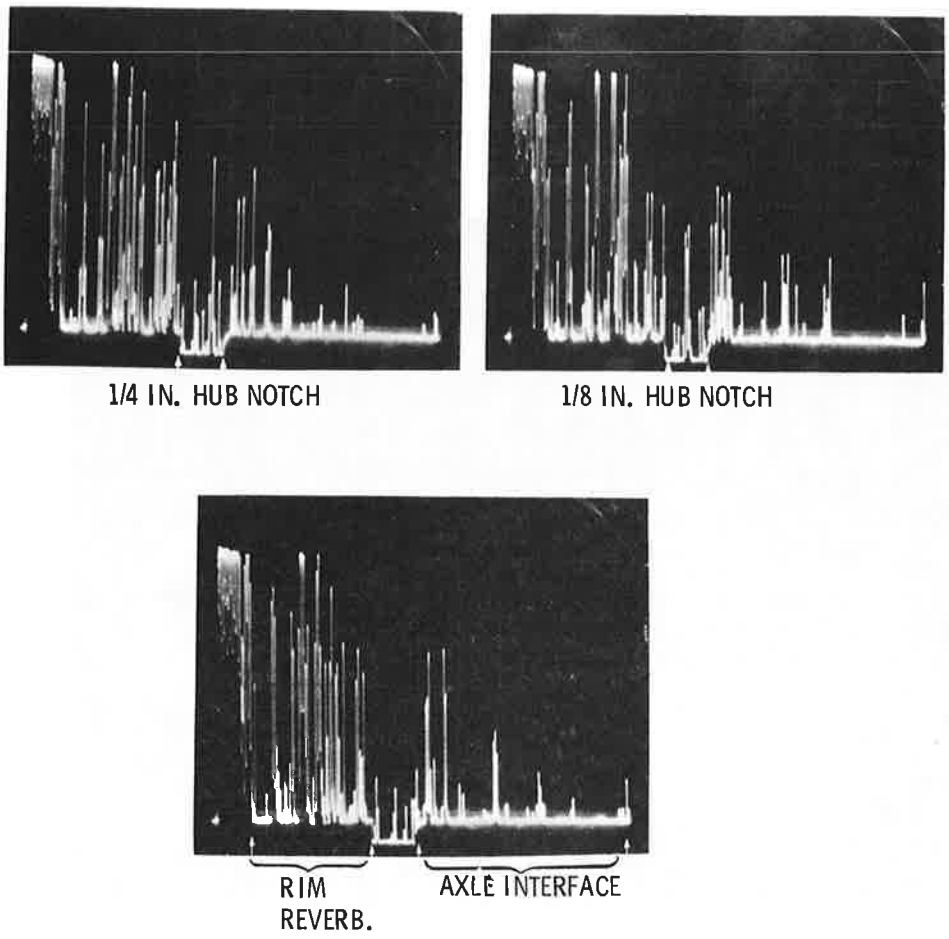

NOTE:

Gain increased by approximately 50% over the setting shown in Figure 25.

Figure 26. Relative Longitudinal-Shear and Background Responses for Test Frequencies of 1 and 3 MHz from 1/4-Inch FFN2 Hub Notch in the M-33 Wheel - Gain Setting Increased

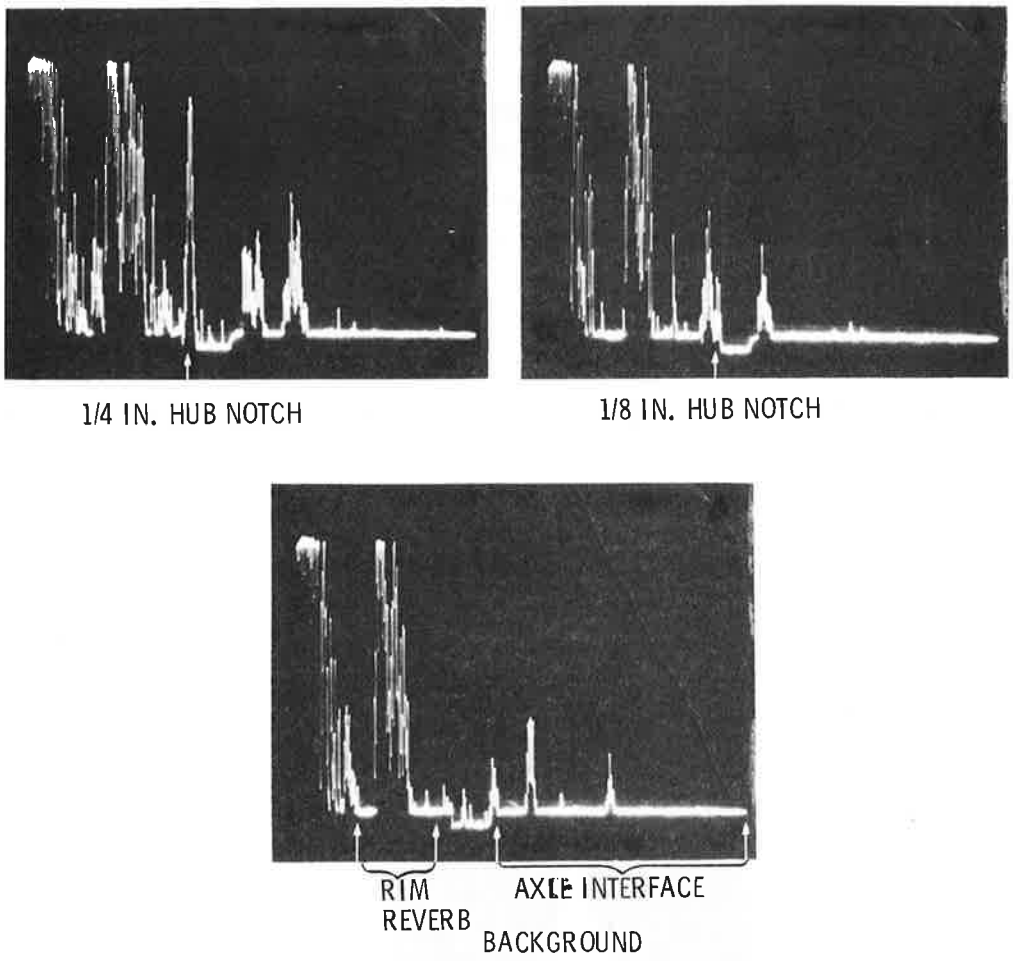

Figure 27. FFN2 Hub Notch Responses in the M-33 Wheel, Obtained by Using a Modified Test Procedure

in Figures 25 and 26; it also operated at a slightly lower frequency, 0.9 MHz rather than 1 MHz. The $\frac{1}{4}$-inch deep FFN2 hub flaw is well separated from the noise. The flaw response was a single pulse with no shear multiples present. The lack of shear multiples, which were most sensitive to the small flaws in the previous tests, was the basic reason for the relatively low sensitivity on this wheel. The responses beyond the gated area (indent in the baseline in Figure 27) were reflections from the hub bore (axle not installed).

The shape of the parabolic plate CJ-33 wheel (see Figure 28) presents a different inspection problem. The rim-to-plate transition is more gradual than for the straight plate wheels. For this type of wheel, the transducer must be placed as close as possible to the flange; results of this test are shown in Figure 29. Gain settings for FFN2 flaws were exactly the same as that used for the straight plate wheels in Figures 21 through 23. The gain for BFN1 rim flaws was approximately 30 percent greater than that used for

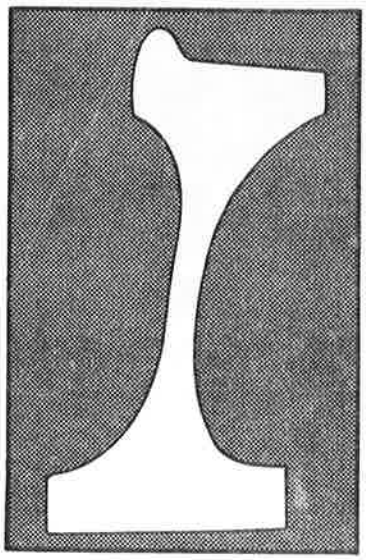

Figure 28. Typical Configuration of a Parabolic Plate Wheel

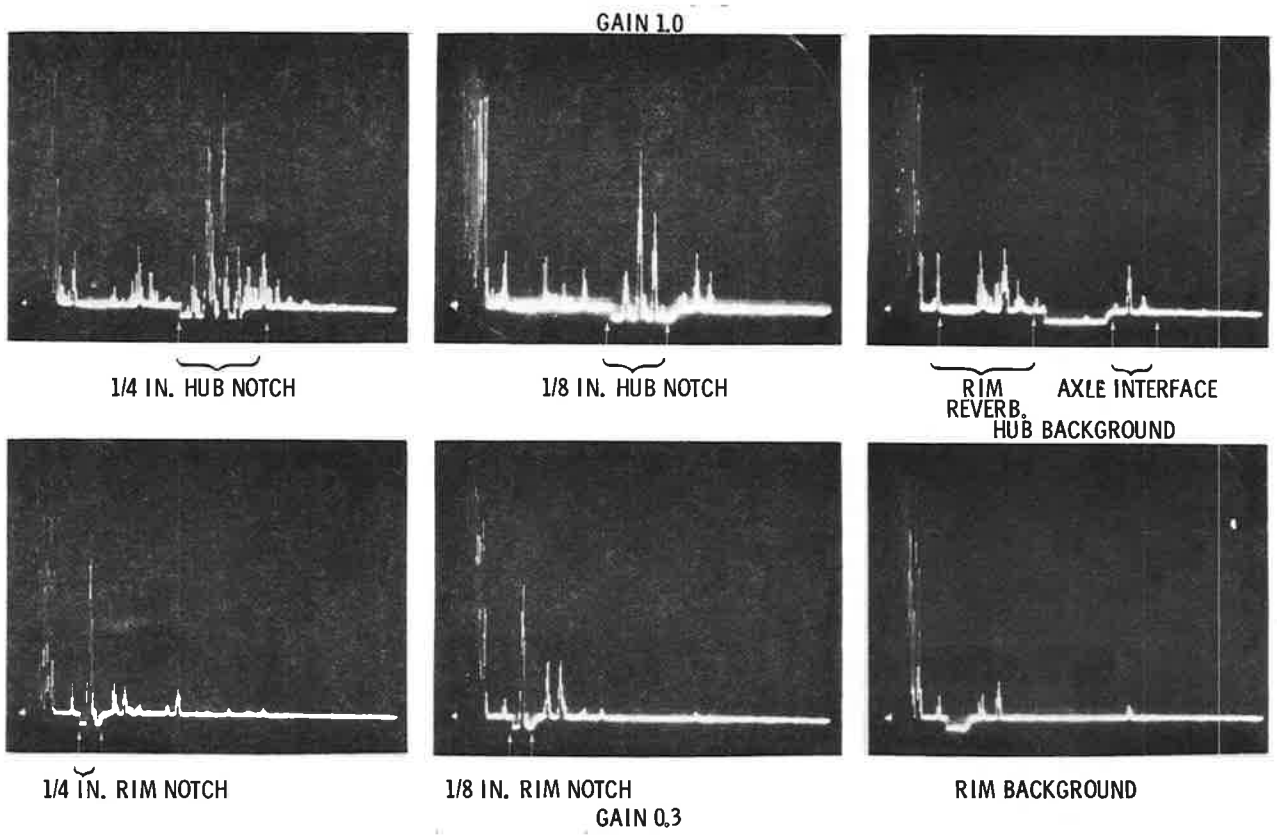

NOTES:

1. Gain for FFN2 Hub Notches is the same as for tests shown in Figure 19.
2. Gain for BFN1 Notches is approximately 30% of that used for FFN2 Hub Flaws.

Figure 29. Longitudinal-Shear Signal Response from Standard Notches in the Cast Parabolic Plate JC-33 Wheel

the straight plate wheels. The flaw sensitivities shown in Figure 29 are very good and comparable to the straight plate wheels.

The tread wear pattern of a used wheel, with its influence on coupling efficiencies and incident angle, was considered to be an important factor in the initial development stages of this program. It was found, however, that transducers 0.5 to 0.75 inches wide were not seriously affected by the wear conditions encountered on the four used wheels. The tread and flange profiles of the four used wheels are shown in Figure 30. None of the four wheels are condemnable for rim thickness or flange height. The J-33 wheel was the most severaly worn of the group and presented no particular inspection problem. However, it would be desirable to evaluate more severely worn wheels. It is not expected that wear will present a serious limitation unless the tread is severely cup-shaped in the measurement area. The most serious condition will result in the case of the parabolic plate wheels where the transducer is placed very near the flange. In this case, a sharp curvature in the tread will change the incident angle of the ultrasound at the rim fillet and will most likely require the transducer be placed closer to the center of the tread for best detection.

In a manual inspection procedure, an edge guide would be provided to assist in locating the best detection position on the tread. The guide would be adjusted to allow free movement of the transducer from the flange to approximately 2.5 inches from the front face. Indications which would fall within the gated region and exceed a preselected amplitude level would be evaluated and rejected, if warranted. The inspection area would be limited to this region, to minimize the probability of spurious rim reverberation indications. It was found, with the exception of the 2-wear M-33 wheel, that no spurious signals fell within the gated region, when the inspection area was limited in this manner.

Maximum response amplitude from a flaw is obtained when the flaw is oriented normal to the incident sound beam. Therefore, this test is limited to flaws which are principally circumferential. This condition is satisfied by almost all flaws which initiate in the plate region. As these cracks grow larger, many tend to

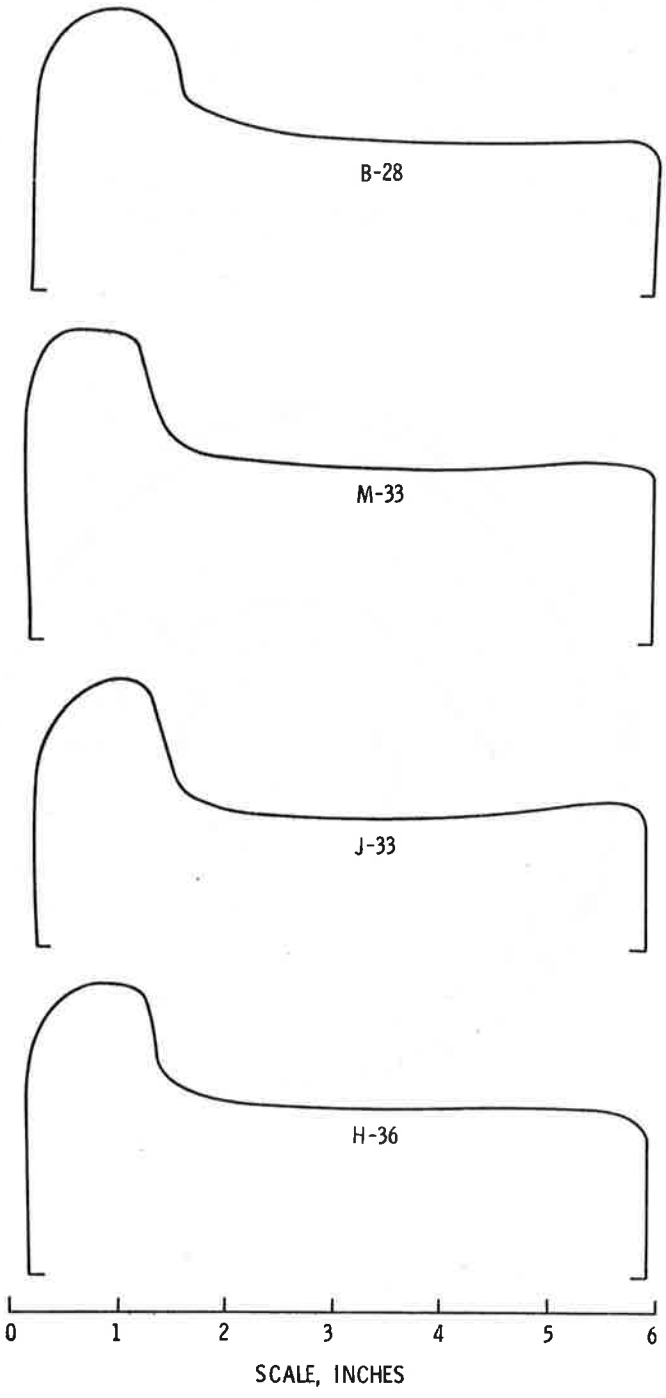

Figure 30. Tread and Flange Profiles of the Four Wheels Used in Testing

deviate from the circumferential. However, due to their large size, they will still yield a detectable signal such as the crack in the mate wheel to the J-33 standard wheel. This crack, sketched in Figure 31, extended through the plate and was approximately 20 inches long. A response amplitude greater than that produced by $\frac{1}{8}$-inch deep reference notch was obtained over the entire length of the flaw.

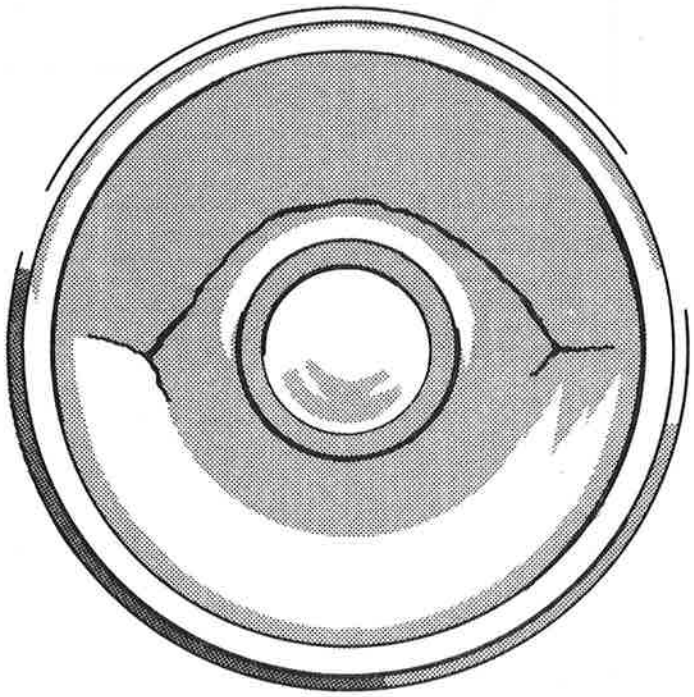

Figure 31. A Sketch of the 20-Inches-Long, Through-Plate Crack in the Mate J-33 Wheel

The relationship between response amplitude of the reference flaw and the circumferential position of the transducer relative to the flaw was also evaluated. This was accomplished by using a 1-MHz, 1 inch long by 0.5 inches wide transducer placed directly

over the 1.5-inch long reference notches and measuring the circumferential distance that the transducer could be displaced before the response signal became reduced to slightly-above the noise level. The total displacement or detection span is a measure of the effective included angle of the transducer for a given flaw, and it is an important parameter is determining the detection probability for automatic testing procedures. The circumferential detection spans for the FFN2 flaws were 4.75 inches and 3.5 inches respectively, for $\frac{1}{4}$ and $\frac{1}{8}$-inch deep, 1.5-inches long notches. Responses from BFN1 notches fell off more rapidly, due to the large variation in incident angle over the shorter path length. This was partially offset by the larger amplitude of signals from BFN1 notches. The detection spans for BFN1 notches were 4.0 and 3.25, respectively, and $\frac{1}{4}$ and $\frac{1}{8}$-inch deep notches, 1.5 inches long. The span width could be extended with a longer transducer, the gain in span being directly proportional to the increased length of the transducer.

4. EVALUATION OF TESTS AND METHODS

4.1 DISCUSSION OF TEST RESULTS

In comparing the test results obtained using the Lamb wave technique and the more conventional Longitudinal-Shear technique, we have concluded that the Longitudinal-Shear technique is the most suitable method. This conclusion was based on the following observations:

- The Longitudinal-Shear technique exhibited a much higher signal-to-noise ratio.
- The Longitudinal-Shear technique was much less sensitive to plate thickness variation.
- The shorter pulse used in the Longitudinal-Shear technique substantially reduced near-surface dead time which, in turn, greatly increased the detectability of BFN1 rim fillet flaws.
- Lamb waves were not generated in the rim fillet area; consequently, the higher frequency of the Longitudinal-Shear method was much more effective for the detection of BFN1 rim fillet flaws.
- The constant propagation velocity of the Longitudinal-Shear technique allowed the use of fixed-time acceptance gates and greatly aided in flaw location.

The sensitivity of any ultrasonic test is principally determined by the signal-to-noise ratio, flaw area, and the wavelength of the incident ultrasonic wave. The size of the reference flaws machined into the test wheels was based on our best estimates of the sensitivity of Lamb waves to this type of defect. Better than expected sensitivity was achieved by using the Longitudinal-Shear technique. In the absence of specific measurements, we can make some estimates of the expected minimum detectable flaw sizes for the Longitudinal-Shear method. These estimates are based on test results shown in Figures 21 through 25 and the response to notches

in the flat reference test plate, Figures 13 through 15. The response from the smallest three flaws (0.15, 0.1 and 0.2 inches deep) in the flat test plates (see Figure 14) is linear and directly proportional to flaw area. This is, the response decreased by approximately $\frac{1}{2}$ for a corresponding reduction in notch area. For flaws smaller than the active area of the transducer, flaw area is more important than the principal dimensions of the flaw, provided the smallest dimension is on the order of $\frac{1}{2}$ wavelength or more. The estimate of minimum detectable flaw size is made by assuming flaw response is linear with flaw area and by determining the minimum signal which can be separated from the noise background.

In a portable or hand-held test, where the operator would have control over the gate width and poisiton, gain setting and transducer position could use some judgement to separate actual flaws from spurious indications; and the minimum detectable flaw would be smaller than could be achieved by an automatic test system where the test parameters must be held constant. The larger response amplitude of rim flaws compared to hub flaws will also yield a lower detection threshold for rim flaws.

Based on test results, it is our best estimate that for a portable test system the minimum detectable flaw sizes would be on the order of:

- x 0.015 inches^2 for BFN1 rim fillet defects,
  for example: 0.07 deep by 0.22 inches long for a 3-to-1 length-to-depth ratio;
- x 0.030 inches^2 for FFN2 hub fillet defects,
  for example: 0.01 deep by 0.3 inches long.

Minimum detectable flaw sizes for an automatic system, where a compromise transducer and gate position must be used, would necessarily be greater that that of the manual test system. We estimate that flaws would need to be approximately 50 percent greater than the flaws for a manual system, to ensure reliable detection by an automatic test system. Minimum detectable flaw sizes are estimated to be approximately 0.022 inches^2 and 0.045

inches^2 for rim and hub flaws, respectively. This would be, for example, for a 3-to-1 length-to-depth ratio, 0.09 deep and 0.25 inches long for BFN1 defects, and 0.125 deep by 0.36 inches long for FFN2 defects. It is expected that these test sensitivities could be obtained on all of the tested wheels, with the exception of the 2-wear M-33 wheel.

These minimum detectable flaw sizes are greater than the minimum critical crash length of 0.16 inches for a stress level of 55 ksi, reported by Carter and Caton[16] for Class U and C wheels, but are close to the flaw sizes reported for Class B and A wheels, 0.25 and 0.5 inches long, respectively. A survey of failure reports contained in the same report (Reference 16) lists the critical crack sizes in 18 plate fractures. Of the seven reported failures at the rim fillet, all exceeded the projected sensitivity of the pulse echo technique. Of the eleven reported hub fillet failures, nine exceeded the minimum detectable flaw for manual inspection, while eight exceeded the estimated detection level for an automatic test. In addition, several of the cracks reported were arrested before they resulted in total failure of the wheel. These cracks were 10 to 20 inches long and similar to the one shown in Figure 31. These wheels would have, no doubt, eventually failed completely, if left in service. They would, however, have been easily detectable by an automatic test system.

Admittedly, this is not a statistically definitive projection of the probability of detecting defective wheels before they result in a total failure. However, it does indicate that a large portion of defective wheels in service can be detected. A comprehensive analysis of available failure data and further efforts to firmly establish the limits of flaw detectability would be required to establish the detection probability and cost effectiveness of this test method.

4.2 INSPECTION SYSTEM CONCEPTS

Concepts for the application of the pulse-echo technique for manual and automatic testing systems are described in the following paragraphs. These concepts are considered to be the preferred

embodiment of the technique at this time. However, further development may yield more suitable system configurations. These concepts are provided to supply a basis for evaluating the potential applicability of the testing technique.

4.2.1 Manual Techniques

In the present state of development, a Manual Pulse-Echo technique could be applied in the field, with a minimum of further development. It is felt that the technique would be suitable to a wide range of wheel sizes and configurations, and could be reliably applied by operators with a minimum of training.

Commerically available portable or chest-pack-type, ultrasonic flaw-detection instruments could be used for this test. An instrument with dual gate capability (with sonic and visual alarms) for rim and hub flaws, would be required, and a distance amplitude correction (DAC) control would also be a desirable feature; several commerical instruments are available with the desired features offered as options. These instruments are battery operated and offer a high degree of portability.

Suitable transducers are also commerically available. The transducer coupling shoe described in Appendix A must, however, be designed to fit this particular application.

In the wheel shop, the manual technique could be applied on mounted or unmounted wheels (preferably mounted). The only facility requirement is the ability to rotate the wheel for access to the entire circumference of the tread.

Application of this test to wheels mounted under a car is complicated by the fact that only 40 to 60 percent of the tread surface is accessible for inspection. Movement of the car would be required for 100-percent inspection of the wheel. Such movement may be required to confirm the presence of a defect detected by an automatic test system, the defect being not visually apparent. The safety of the inspector is also an important consideration in this case, since the inspector would be standing close to the wheel with his hand on the tread surface. The "blue flag rule"[17] must be

imposed to preclude movement of the car while the inspector is at work.

4.2.2 Automatic Test Systems

The following discussion pertains to a system concept and its capabilities for the automatic detection of plate defects in wheels under moving cars. One proposed system uses a series of transducers mounted in a specially designed section of rail, with each transducer inspecting a portion of the wheel as it rolls over that unit. A second system concept using transducers mounted on a travelling carriage is presented as an alternative approach, but is not recommended because of its many limitations.

4.2.2.1 In-Rail System - A conceptual sketch of the in-rail system in Figure 32. The spring-loaded transducers are mounted in a fluid-filled boot. As a wheel rolls over the assembly, the transducer and boot are forced against the treat; the transducer is self-aligning. The transducer face is curved to provide maximum contact area on the tread surface. The exact curvature of the transducer would be determined by experiment to provide the most efficient coupling over the range of wheel sizes to be tested. The outer surface of the boot is kept wet by a small jet spray triggered before the arrival of the wheel, to assure good coupling to the wheel. A guide shoe or rail is provided for lateral positioning of the transducer. The lateral positioning is accomplished before the transducer contacts the tread. Further experiments will be required to determine the most suitable transducer position to compensate for the ranges of wheel configurations, tread and back rim wear patterns which will be encountered. The transducer assemblies are mounted in two specially designed 11 to 12-foot-long rail sections. An estimate of the detection probability can be made for this system if we make two assumptions concerning the circumferential detection span of the transducers. First, we assume that a FFN2 hub defect over a 4-inch circumferential span, and secondly,

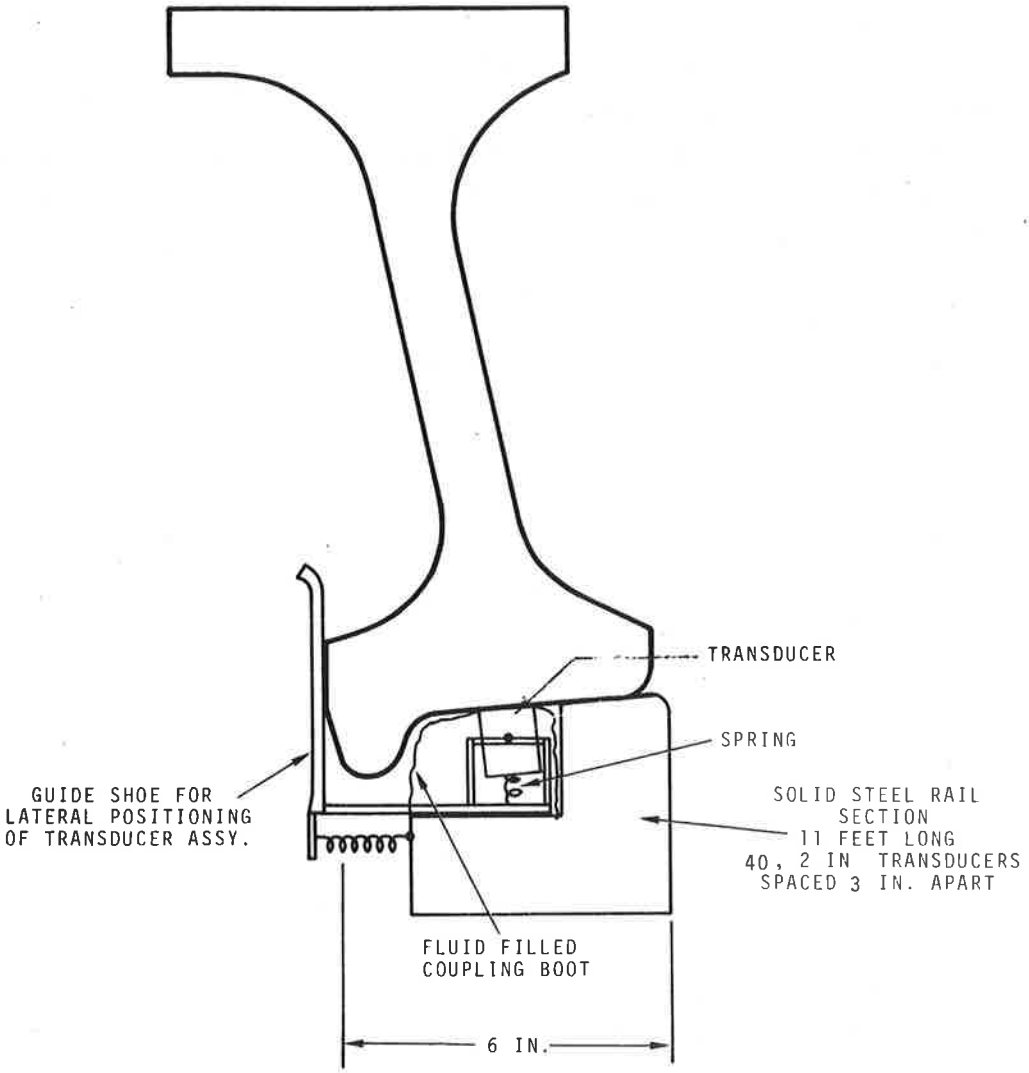

Figure 32. Automatic In-Rail Inspection System Components - Conceptual Diagram

that small flaws, down to the detection limit, will be detected only when they are directly over the transducer.

Figure 33 is an estimate of the detection probability, based on the above assumptions, for transducer spacings of 3, 4, and 8 inches. The vertical portion of the curves in Figure 33 represents the expected minimum detectable flaw size. The plateau region corresponds to the probability that a small flaw will fall within the length of the transducer. As the length and depth of a flaw is increased the received signal increases, and it can be detected over a greater circumferential distance. The probability that a substantial portion of the flaw will fall over the transducer also increases with flaw length, resulting in a higher detection probability. A detection probability of 1.0 is achieved when the length of the flaw is sufficient to guarantee that some portion of the flaw will fall within the detectable range of at least one transducer. The smaller spacing obviously yields the highest detection probability. The total number of transducers will depend on the spacing. For spacings of 3, 4 and 8 inches, respectively, a minimum of 40, 30 and 15 transducers in each rail would be required to inspect 38-inch diameter wheels.

The electronic equipment required for this type of inspection system would be relatively complex, but it is within the present state of the art. If the test rail is 120 inches long, containing 40 transducers spaced 3 inches apart, wheels up to a 38-inch diameter can be inspected. The test rail would then consist of four electronically independent sections containing 10 transducers. No more than one wheel at any given time will be present on any one 30-inch section, because axle-to-axle spacing is always greater than 30 inches. The 120-inch test rail can accommodate two or more wheels at the same time, each of the four 30-inch sections being electronically independent.

Each of the four independent sections can be controlled by one transmitter-receiver through a 10-channel multiplexer. A transmitter repetition rate of 5 KHz results in an effective repetition rate of 0.5 KHz at each transducer. At a train speed of 10 mph (or 176 in./sec), each of the 2 inches long transducers would be

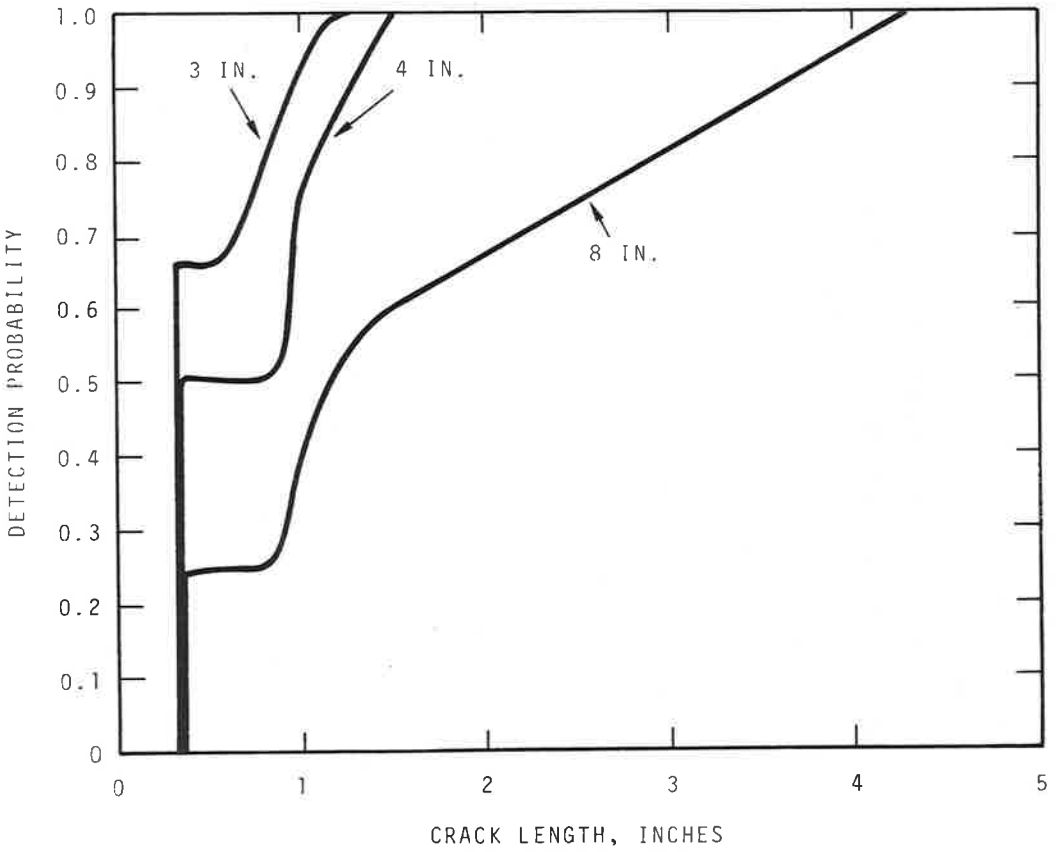

Figure 33. Projected Detection Probability Vs. FFN2 Hub Fillet Crack Length for In-Rail Systems with Transducer Spacings of 3, 4, and 8 Inches

pulsed at least five times, as the wheel passes over the transducer. Speeds up to 20 mph could be accommodated by doubling the pulse repetition rate. Automatic paint markers would be provided for each group of 3 to 4 transducers, to identify defective wheels and to mark the approximate circumferential location of the defect. A duplicate 4-channel system would be provided for each test rail.

It is anticipated that this type of system would be installed in a hump yard. It would be desirable to incorporate an automatic car identification system so that a car with a defective wheel could be shunted onto a repair track. One simple method would be to count the wheels as they pass over the test rail. A counter would be installed for each of the four test sections in each rail. When a defective wheel is encountered, the sequential number of the wheel in that test section of the rail would be relayed to the hump-yard switching control panel. A counter placed near the top of the hump would signal the presence of the defective wheel and cause the car to be shunted.

4.2.2.2 Carriage System - A second automatic inspection system concept also was considered. In this system, 16 transducers (one for each wheel of the car) would be mounted on a small carriage placed between the two rails. The transducers would be positioned against the tread surface and the entire assembly would follow the car one complete revolution of the wheel; the transducers would then be retracted, and the carriage mechanically repositioned to inspect the next car. The basic advantage of this type of system would be its higher detection probability for flaws less than 1 inch in length. Further consideration of this type of system was dropped in fabor of the in-rail system previously described, for the following reasons:

1. It would be a highly complex mechanical system susceptible to mechanical and environmental damage which could severely limit its reliability.
2. The capital and maintenance costs of the mechanical system would be considerably higher.

3. Inspection speed would be limited to the low-speed range of 1 to 2 mph.

4. The 25 to 30 percent increase in detection probability for flaws between 0.4 and 1.0 inches long does not appear to justify the added system cost and complexity.

4.2.2.3 In-Rail Test Advantages and Cost Estimates - The advantage and capabilities of the in-rail automatic test can be summarized as follows:

1. Wheel plate defects longer than 1 inch can be reliably detected.

2. Test speeds of 10 mph or more are possible, so that interference with normal operating procedures is kept to a minimum.

3. The system is completely automatic, requiring one operator to monitor system operation and to perform periodic maintenance and calibration. The system may be capable of operating unattended for extended periods. It is, however, recommended that an operator be present for at least one shift per day.

The capital cost of an automatic in-rail inspection system would be substantial; however, this cost could be small compared to the cost of a serious accident resulting from a wheel failure. The operating cost of the system would be modest requiring one operator and periodic maintenance costs. The cost per wheel inspected would depend on the number of wheels inspected per day. It is not possible to predict system and operating costs exactly. We can, however, make some estimates. If we assume a system could be installed for less than $150,000, and amortized over a 10-year period, this would be $15,000/year, a sum less than the average cost per accident,[1] or $40/day.

If we further assume that the system could be operated and maintained for $100/day, the total cost would be less than $150/day. Based on a rate of 1,000 cars/day this would amount to an

inspection cost of less than one cent per wheel. Should the system prove to be reliable enough to operate unattended for extended periods of time, the inspection cost per wheel would be substantially reduced.

A study of traffic patterns and failure rates would be needed to establish the number and most suitable locations for these test systems. If, for example, ten strategically located installations could assure adequate coverage, the total estimated yearly cost of operation would be approximately $550,000 or 12 percent of the estimated $4.5 million annual loss resulting from cracked plate wheel failures.

5. CONCLUSIONS AND RECOMMENDATIONS

5.1 GENERAL CONSIDERATIONS

Because of the test results obtained, it is felt that the Longitudinal-Shear Wave technique is the most suitable method and will be applicable to a large range of wheel sizes and configurations. This test method shows considerable promise and apparently warrants further development. It is capable of detecting a substantial portion of the plate cracks which occur in service before they result in catastropic failure of the wheel. It would constitute a substantial improvement over the present visual detection methods.

There is also considerable economic justification for proceeding with the system development. On the basis of projected operating and inspection cost estimates, it appears that the automatic testing system could be very cost effective in detecting defective wheels and reducing the number of costly accidents.

5.2 MANUAL SYSTEM

5.2.1 Recommendations for Development

The first recommended effort is to complete the development of the manual inspection method. The manual method could be used to evaluate the conditions of wheels before remounting or turning; to inspect wheels of cars undergoing repair or refurbishment; to perform field inspections on groups or classes of wheels which have experienced high failure rates, and to verify defects detected by an automatic test system. More importantly, the manual system would provide the basis and experience required for development of the automatic test system.

We recommend that the following tasks be pursued to complete the development of the manual inspection technique:

- Establish minimum detectable flaw sizes;
- Complete development of transducers suitable for field use;

- Design field evaluation program to test the concept on the largest number of wheels possible;
- Complete development of inspection and calibration techniques;
- Finalize instrument design.

5.2.2 Minimum Flaw Size

Establishing minimum detectable flaw sizes is important for two reasons. First, it is necessary to establish a basis for setting inspection limits. Second, it is desirable to obtain a measure of the test effectiveness as compared to the critical crack size. It is not assumed that the test will be capable of detecting cracks as small as the minimum critical crack lengths reported by Carter and Caton.[16] However, based on the wheel failure reports published in Reference 16, it appears that a majority of the cracks occurring in service can be detected before they cause wheel failure. The actual detection limit would be established by machining a series of small notches in existing wheels and evaluating the signal response from each notch. A fatigue crack will always appear smaller than the same size standard notch, due to its irregular surface; its orientation may be less than optimum, and the crack surfaces may be pressed tightly together. It is not practical to use fatigue cracks as test standards; however, experiments should be performed to establish a correlation between the responses received from fatigue cracks and standard notches of the same size.

5.2.3 Transducer Development

Further transducer development is required to provide a sturdy and reliable transducer for field applications. The transducer design recommended for further development is shown in Appendix A. This unit uses commerically available transducers and a replaceable coupling shoe which also incorporates a liquid couplant supply that provides consistent coupling film beneath the transducer. Coupling shoes of various radii would be provided along with an adjustable edge guide for proper positioning of the transducer.

5.2.4 Field Evaluation

The purpose of the field evaluation is to determine the effectiveness of the test method under a wide range of wheel sizes, configurations and wear conditions. It should be anticipated to inspect 200 or more wheels of various types. It also should be attempted to locate several wheels already known to be defective. The majority of these tests should be performed in wheel shops of cooperating railroads. The results of each inspection should be documented and evaluated. On the basis of this information, an accurate determination of the effectiveness of this test method could be established. The testing should also provide the data needed for the development of automatic test systems.

5.2.5 Calibration and Test Procedures

The use of full-size wheels as calibration references would be grossly inconvenient for field or wheel shop inspections. Calibration techniques and test procedures need to be developed in conjunction with the field evaluation described above.

5.2.6 Instrumentation

We recommend the use of commercially available portable ultrasonic instruments for the field evaluation and development portions of the program. After completion of the field evaluation, the feasibility and design requirements of a single-purpose instrument capable of performing the test and giving simple go/no-go indications could be established. The effort should be aimed at providing the simplest test possible which could be performed by relatively unskilled operators.

5.3 AUTOMATIC SYSTEM

The considerations of cost effectiveness constitute one of the most important factors that govern the acceptance of a test procedure by industry. The cost effectiveness of automatic test methods could be established on the basis of field evaluations, available failure data, and the projected cost of the test system.

A projection of the minimum number and possible locations for automatic test systems should also be made in order to achieve optimum cost effectiveness.

It is recommended that, in the second phase of the continued development, the automatic inspection concepts be evaluated. This would include the development of a prototype inspection system consisting of ten transducers mounted in a short test rail, as well as the associated electronic system. The electronic system could be a commercial receiver-transmitter unit connected to a ten-channel switching network. This system would be evaluated in the laboratory for various wheel types and flaw sizes, to determine its sensitivity and detection probability, and to establish an estimate of the maximum test speed.

The third phase of the program would include the development and fabrication of a system for installation in a test track, to demonstrate system accuracy and applicability under operating conditions. It is expected that a determination of the commercial feasibility of full-scale systems would be established during this stage of development.

Such a demonstration of the system's feasibility and capabilities should result in acceptance and application of this test system by the industry. The implementation of this system, coupled with existing techniques for the detection of tread cracks,[18] would substantially reduce the occurrence of accidents resulting from wheel failures.

APPENDIX A
ULTRASONIC TRANSDUCERS

Several types of ultrasonic transducers were employed during this investigation. This appendix describes each of these transducers and discusses the relative merits of each type. The transducer and coupling shoe configuration considered most suitable for further development is also described.

The basic suitability of any test is determined by the signal-to-noise ratio. That is, the relative amplitude of the detected flaw signal versus all other detected signals from other sources. The principal sources of noise in this test are random scattering from grain boundaries and reflections resulting from the geometrical configuration of the wheel. Random grain scattering increases with test frequency as the wave length approaches the size of the grain. In most cases the influence of geometrical reflections is minimized by the use of acceptance gates; they do, however, reduce the total amount of energy available at the flaw. The amplitude of the detected flaw signal is principally determined by the magnitude of the incident energy, the size of area of the flaw relative to the incident beam area, the wave length of the ultrasonic wave, and the orientation of the flaw. Maximum flaw signal amplitude is achieved when the flaw is oriented perpendicular to the incident beam, the principal dimensions of the flaw are large, as compared to a wave length, and the area of the defect is a substantial portion of the incident beam area.

Transducer selection for this application was a compromise of several factors. To achieve maximum sensitivity, we preferred to use a beam no larger than the plate thickness and the highest possible frequency consistent with material attenuation over the required path length. Frequencies of 1 to 3 MHz are the most suitable. Transducer widths from 0.5 to 0.75 inches yield beam widths of 1 inch or less at the rim-to-plate transition. The narrow width of the transducer also aided in efficient coupling to worn tread contours. Transducer lengths of 1 to 2 inches were used.

The direct contact coupling technique, as opposed to immersion, was considered to be most applicable for two reasons. In an immersion test, approximately 88 percent of the energy is reflected at the liquid-steel interface. Substantially greater usable energies are achieved using the direct contact technique. Secondly, to prevent liquid path multiples, a liquid path of up to 5 inches would be required for immersion testing. This would considerably complicate the testing procedure.

To achieve efficient coupling to the cylindrical tread surface, required a shaped transducer or a flat transducer with a shaped coupling shoe. Two shaped transducers were evaluated. The piezo-electric elements were ground to match the curvature of the 33-inch wheel and had a resonant frequency of 0.6 MHz, but were also usable at the third harmonic (1.8 MHz). These transducers were 1.0 inch wide by 1.5 inches long and 0.5 by 1 inch long, with the curvature in the long dimension. These two transducers were used principally for Lamb wave testing and efficiently coupled sound into the wheel. However, they were considered to be impractical due to the fragile nature of the elements and electrodes and because of the difficulty in attaching a good, wear-resistant face to the shaped element.

Three materials were considered for the coupling shoe: lucite, alumina, and lavite (a fireable ceramic which is easily machined in the green state). Alumina is the hardest of these materials and would be most suitable to prevent wear; however, it was difficult to shape and had a high acoustic impedance* of 36 gm/cm^2 sec x 10^5. The high acoustic impedance of alumina relative to the glycerine couplant (2.42) results in large reflections at the interface and long-term reverberations in the shoe. Lucite on the other hand, with an acoustic impedance of 3.16, coupled sound more efficiently and was less affected by variations in couplant layer thickness. Lucite, however, did not wear well when used on rough surfaces. The Lavite material, with an acoustic impedance of 10, was a suitable compromise between coupling efficiency and wear resistance.

*Acoustic impedance is the product of density and velocity.

The 1, 2, and 3-MHz transducers used for the pulse echo testing of the wheels were fabricated by using permanently bonded lavite shoes. Each of the shoes was 2 inches long, 0.75 inches wide and approximately 0.1 inch thick at the top of the radius. The 1 and 3-MHz units were ground to match the curvature of a 33-inch wheel, while the 2-MHz unit was ground to match the curvature of the 28-inch wheel. The transducer elements were 1 inch long and 0.75-inches wide lead zirconate titanate material. The elements were bonded to the coupling shoes, using a thin layer of epoxy. Back surface damping was provided by a 1.5-inch layer of tungsten-loaded polyurathane.

The performance of these transducers was adequate for our purposes. However, several improvements could be made in their capabilities. Figure A-1 is a sketch of a transducer assembly that is proposed for the manual inspection system. This unit would utilize commercially available transducers and a replaceable wear shoe. For the manual inspection technique, a 2-MHz transducer, 0.75 by 1 inch long, is recommended.

The 1-MHz transducer ground to match a 33-inch wheel was used on all three wheel sizes, to determine the relative response of defects in each wheel and to demonstrate their suitability for automatic testing procedures. It is recommended that a replaceable coupling shoe be provided for each wheel size to be manually tested. This improves the inspector's ability to align the transducer and maintain a relatively thin and consistent coupling film. The use of pressure or gravity-feed couplant supply would also aid in assuring a uniform couplant layer at the transducer face. The coupling show could be fabricated using lucite, lavite or similar materials suitable for manual inspection needs. Automatic testing procedures will require the more durable types of material, such as lavite.

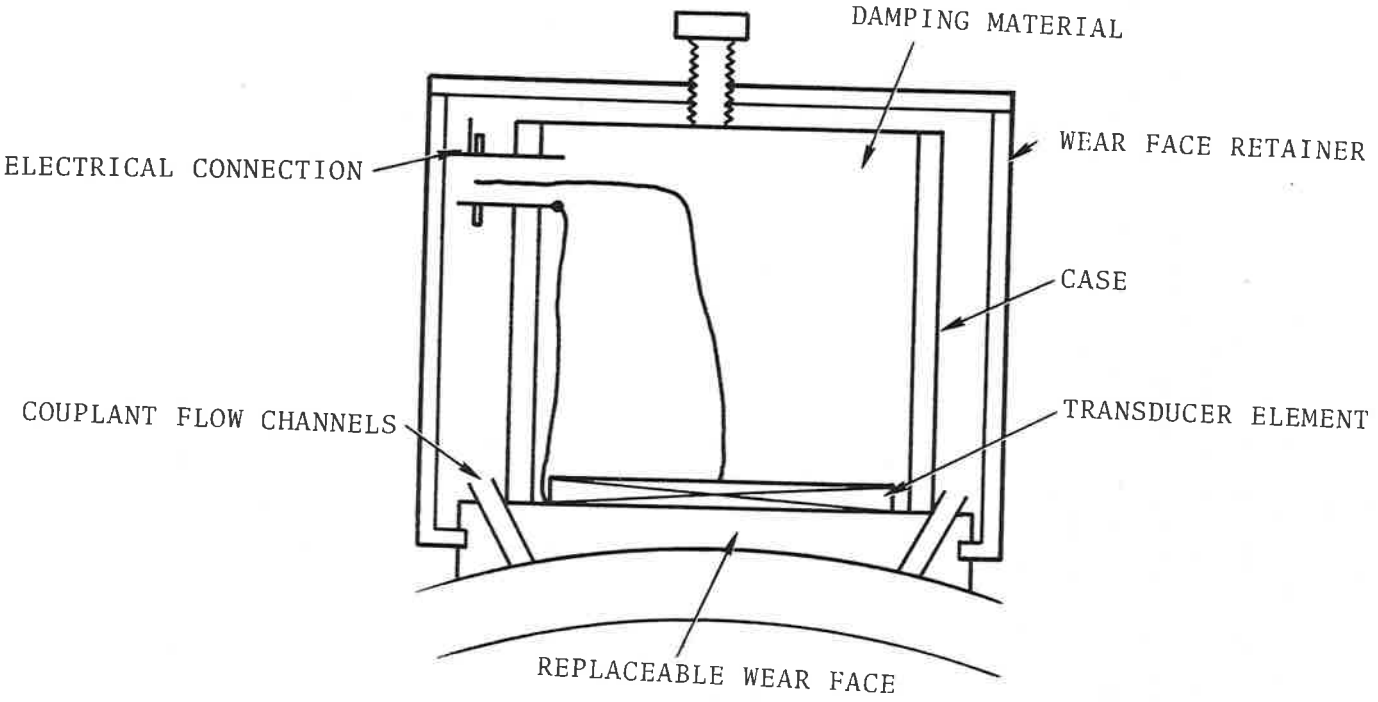

Figure A-1. Transducer Design Proposed for Wheel Inspection System

APPENDIX B
ELECTROMAGNETIC-ACOUSTIC METHODS

The Electromagnetic-Acoustic (EMAC) method is a relatively new means of generating and receiving ultrasound in electrically conductive materials. Recent studies at Battelle Northwest indicate that the EMAC method has good potential for application to many nondestructive testing situations where conventional ultrasonic methods are difficult to apply. The EMAC method has several advantages over conventional ultrasonic test methods. The primary advantage is the absence of a need for an ultrasonic couplant between the EMAC transducer and the test piece. This and other advantages make the EMAC method desirable for many applications where high speeds and/or rough surfaces preclude the use of normal procedures. An evaluation of this technique was performed as a part of this program, to determine the feasibility for the detection of plate cracks.

The basic EMAC inspection system used in our tests consists of a high voltage pulse generator, an EMAC transmit transducer, an EMAC receive transducer, a preamplifier, a filter, and an oscilloscope (see Figure B-1). The EMAC transmit and receive transducers each consist of an electromagnetic coil in the presence of a magnetic field. When the EMAC transmitter is placed over a metal and a pulse burst is applied to the transmitter coil, the flow of eddy currents generated within the metal interact with the magnetic field lines from the transducer, to generate an ultrasonic wave in the metal. The ultrasonic wave travels in the metal to the location of the receive transducer where the particle motion of the metal interacts with the magnetic field lines of the receive transducer, to generate a voltage across the receive transducer coil. The receive signal is amplified, filtered, and presented on an oscilloscope as in conventional ultrasonic systems.

A 300-KHz receiver transmitter pair was used to evaluate the sensitivity of this technique on 0.1 to 0.5-inches deep 1-inch long notches in the standard test plate, in a manner similar to

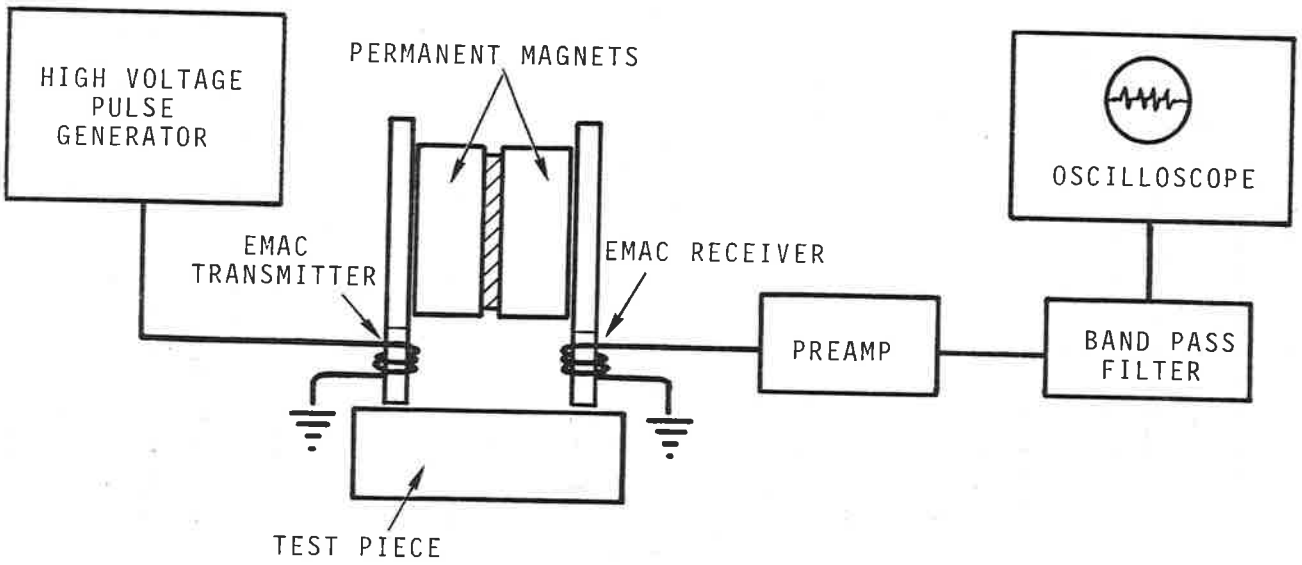

Figure B-1. The Electromagnetic-Acoustic System - Block Diagram

that shown in Figures 9 and 13. The response from these notches is shown in Figure B-2, which compares favorably with that shown in Figure 9. The magnitude of these signals is quite small (in the millivolt range), due to the relatively low conversion efficiency of the technique.

This technique was also evaluated on full-size wheels with little success, mainly because of the small amplitude of the signals and nearly spherical distribution of the energy resulting from the small diameter (0.25 in.) of the probe and the low frequency. The predominant mode of propagation appeared to be a surface wave traveling around the tread of the wheel. As many as 15 complete surface wave circuits around the wheel were detected above the noise level. These were reduced to very low levels by the presence of a surface defect on the tread or flange.

Although the EMAC technique, is not at present feasible for plate crack detection, it may very well become, if developed, a simple and effective method for detecting tread and flange cracks. These applications were not pursued, as they are beyond the scope of this program.

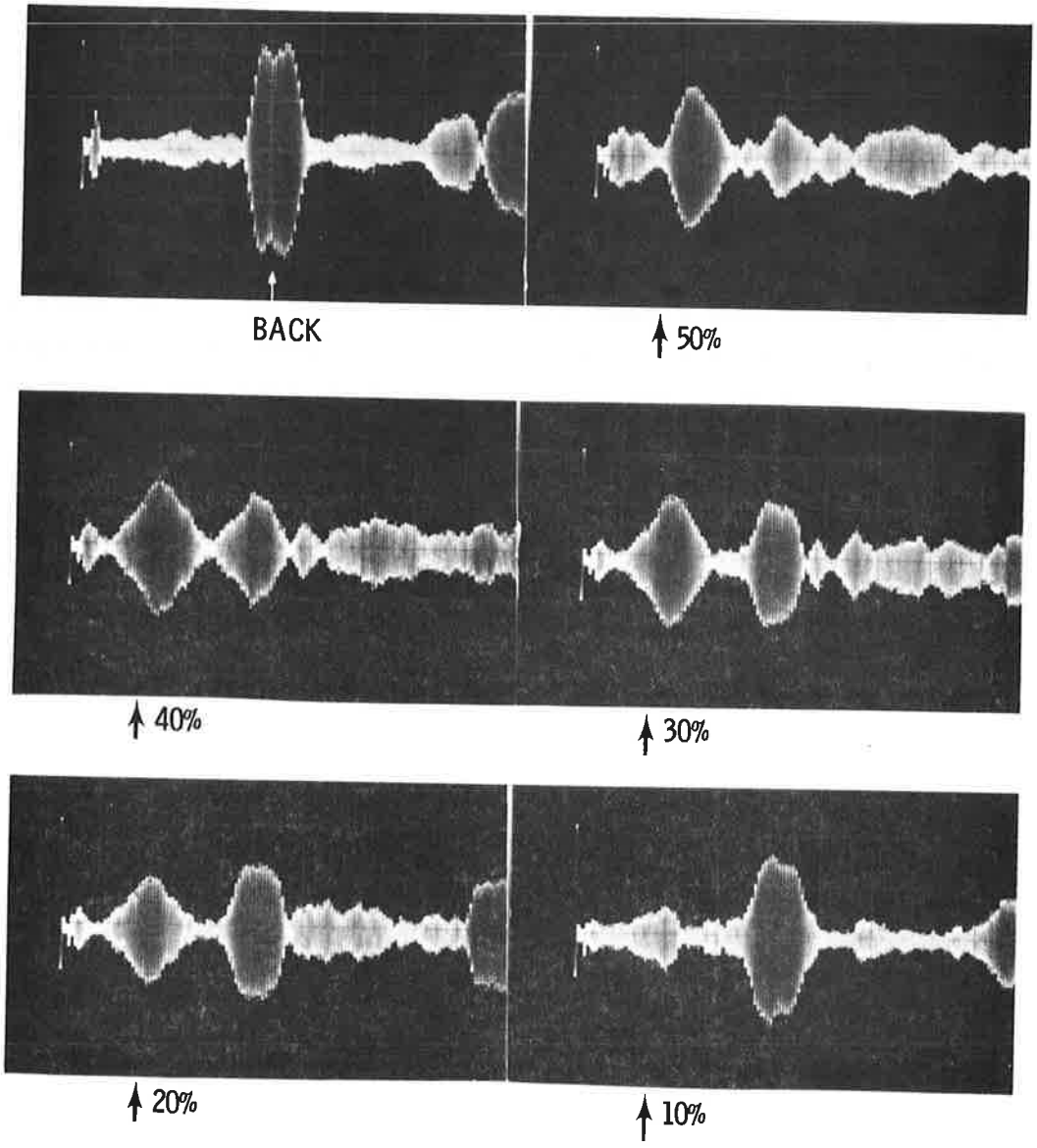

Figure B-2. Signal Response from 1-Inch Long, 0.1 to 0.5-Inches Deep Standard Test Plate Notches, Obtained by Using 300-KHz EMAC Transducers

REFERENCES

1. Accident Bulletin, Federal Railroad Administration, No. 141, 1972.
2. Association of American Railroads Annual Report, Exhibit F, December 31, 1972.
3. D.E. Bray and R.D. Finch, Flaw Detection in Model Railway Wheels, FRA-RT-71-75, University of Houston, Houston, TX, 1971.
4. G.E. Novak and B.J. Eck, "A Three Dimensional Finite Difference Solution for Thermal Stresses in Railcar Wheels," ASME paper No. 69-RR-4, 1969.
5. M. Riegel, S. Levey and J. Sliter, "A Computer Program for Determining the Effect of Design Variations on Service Stresses in Railroad Wheels," Transactions of the ASME, V. 88, pp. 352-362, Nov. 1969.
6. J.P. Bruner, et al., "Effect of Design Variation on Service Stresses," Trans. ASME, 90, B, p. 187, 1968.
7. H. Lamb, "On Waves in an Elastic Plate," Proc. Roy. Soc. London, A93, pp. 114-128, 1971.
8. E. Lahfeldt and E. Holler, "Lamb Waves and Lamination Detection," Ultrasonics, Vol. V, pp. 225-257, October 1967.
9. I.R. Kraska and R.G. Prusinski, Development and Field Evaluation of a Thin Sheet Inspection System, AFML-TR-70-315, General American Transportation Corporation, Niles, IL, April 1971.
10. T.N. Grigsby, "Properties of Lamb Waves Relevant to the Ultrasonic Inspection of Thin Plates," IRE Transactions, Vol. VE-8, No. 1, pp. 69-96, March 1961.
11. I.A. Viktorov, Rayleigh and Lamb Waves, Plenum Press, New York NY, pp. 67-121, 1967.

12. M.R. Redwood, Mechanical Waveguides, Pergamon Press, Oxford, 1960.

13. D.C. Worlton, "Experimental Confirmation of Lamb Waves at Megacycle Frequencies," J. Applied Physics, Vol. 32, No. 6, pp. 967-971, 1961.

14. J. Krautkramer and H. Krautkramer, Ultrasonic Testing of Materials, Springer-Verlag, New York, NY, pp 244-247, 1969.

15. B.T. Cross, Sound Beam Directivity: A Frequency Dependent Variable, TR 70-23, Automation Industries, Boulder, CO, April 1970.

16. C.S. Carter, and R.G. Caton, Fracture Resistance of Railroad Wheels, FRA-ORD-&-D-75-12, Boeing Commercial Airplane Co., Seattle, WA, 1974.

17. Rules 10 & 26 AAR Standard Code of Operating Rules, 1975.

18. "Inspect Wheels in Motion," Progressive Railroading, pp. 50-52, January 1974.